Controlling Error Propagation in Cooperative Communication Networks

Ghaleb Al-Habian

A Thesis
in
The Department
of
Electrical and Computer Engineering

Presented in Partial Fulfillment of the Requirements
for the Degree of Master of Applied Science in Electrical & Computer Engineering
Concordia University
Montréal, Québec, Canada

April 2009

Your file Votre référence
ISBN: 978-0-494-63173-7
Our file Notre référence
ISBN: 978-0-494-63173-7

Abstract

Controlling Error Propagation in Cooperative Communication Networks

Ghaleb Al-Habian

In cooperative communications, error propagation at the relay nodes degrades the diversity order of the system. To combat that effect, we present a novel technique to control error propagation at the relays, which is implemented in the context of a distributed turbo code. In the presented technique, the relay calculates the log-likelihood ratio (LLR) values for the bits sent from the source. These values are subjected to a threshold to distinguish reliable decoded bits. The relay then forwards bits that are deemed reliable and discards bits that are not, resulting in less errors propagating to the destination. We develop upper bounds on the end-to-end bit error rate, enabling us to optimize the threshold in terms of the minimum end-to-end bit error rate. We compare our technique with existing techniques to control error propagation, including using only a cyclic redundancy code (CRC) check at the relay, forwarding analog LLR values, and with employing no error control at the relay at all. We demonstrate, via several numerical examples, that the performance of our proposed scheme is superior to all existing techniques.

We investigate the application of this technique to a network-coded two-way relay channel where the relay is assisting two sources simultaneously. We propose two modes of thresholding: at individual bits and at combined bits. We analyze the bit-error rates of both thresholding modes and optimize the threshold for both. We show significant gains using thresholding over an unthresholded network-coded system. Based on system simulations, we conclude that utilizing separate thresholds yields better results than utilizing a combined threshold scheme.

Their gift is that of unconditional love, trust, and belief...

Dedicated to my dearest mother and father.

Acknowledgments

My sincerest gratitude and thanks go to Dr. Ali Ghrayeb; without his guidance, supervision and endless support this work wouldn't have been possible.

Special thanks to Drs. Mazen Hasna and Adnan Abu-Dayya from Qatar University, their unique outlook was instrumental in shaping this work to its current state.

Thanks to Jeyadeepan Jeganathan, May Gomaa, Pooyan Haghighat, Xiangnian (Beta) Zeng, and Mohamed El-fituri for their continuing assistance and help throughout this work.

Last but not least, sincere regards to all the Department of Electrical and Computer Engineering supporting staff for all their hard work and support.

Contents

List of Figures

List of Acronyms

AF	Amplify-and-forward
APP	*A-posteriori* probability
AWGN	Additive white gaussian noise
BER	Bit error rate
BPSK	Binary phase shift keying
CF	Compress-and-forward
CRC	Cyclic redundancy check code
CSI	Channel state information
DF	Decode-and-forward
DTC	Distributed turbo coding
EF	Estimate-and-forward
LLR	Log-likelihood ratio
MIMO	Multiple input multiple output
ML	Maximum Likelihood
MRC	Maximum ratio combining
PDF	Probability density function
PEP	Pairwise error probability
RF	Radio frequency
SCCC	Serially-concatenated convolutional code

SISO	Soft input soft output
SNR	Signal-to-noise ration
SOVA	Soft-output Viterbi algorithm
WCDMA	Wideband code division multiple access
XOR	Exclusive OR

List of Symbols

$*$	Discrete-time convolution
$\bar{Y}$	Indicates the mean value of random variable Y
$\binom{\cdot}{\cdot}$	Indicates the binomial coefficient
γ_{D_1}	Received-signal-to-noise ratio at the destiantion during the first stage
γ_{D_2}	Received-signal-to-noise ratio at the destiantion during the second stage
γ_{RD}	Received-signal-to-noise ratio at the destiantion from the relay
γ_{SD}	Received-signal-to-noise ratio at the destiantion from the source
$\hat{u}$	The modulated output of the relay
$\Lambda_{\mathbf{u}}$	LLR values calculated at the relay
$\mathbf{b}$	Bold lowercase letters indicate a vector of similarly-named elements
$\mathcal{E}$	Is the general symbol for a statistical event
$\mathcal{Q}(\cdot)$	Gaussian tail function
$\oplus$	Indicates the exclusive-or (XOR) operator
$\Re(\cdot)$	Indicates the real part
d_1	Number of bits in an error word that belong to the first stage
d_2	Number of bits in an error word that belong to the second stage
d_ϕ	Number of bits in an error word that had no contribution from the relay
d_{free}	The free hamming distance of the turbo code

d_C Total number of bits in a transmitted frame that received correct contribution from the relay

d_c Number of bits in an error word that had a correct contribution from the relay

d_E Total number of bits in a transmitted frame that received wrong contribution from the relay

d_e Number of bits in an error word that had a wrong contribution from the relay

d_R Total number of bits in a transmitted frame that received contribution from the relay

d_r Number of bits in an error word that receive contribution from the relay

E_b Energy transmitted per bit

$E_Y[\cdot]$ Indicates the expectation with respect to random variable Y

h_{RD} The fading channel coefficients for the relay-destination channel

h_{SD} The fading channel coefficients for the source-destination channel

h_{SR} The fading channel coefficients for the source-relay channel

N Block length of the encoded information frame in bits

n The discrete-time index

$N_0/2$ AWGN variance per dimension

n_{RD} AWGN noise samples over the relay-destination channel

n_{SD} AWGN noise samples over the source-destination channel

n_{SR} AWGN noise samples over the source-relay channel

$P(\cdot)$ The probability of an event

$p_Y(y)$ The probability density function (PDF) of a random variable Y

r_{MRC} Output of MRC combiner at the destination

R_{c_1} Channel code rate during the first stage

R_{c_2} Channel code rate during the second stage

r_{RD} Recieved samples at the destination from the relay

r_{SD} Recieved samples at the destination from the source

r_{SR} Recieved samples at the relay from the source

T_i Genie-aided threshold, where i equals number of errors allowed to pass

T_Z CSI-based threshold

Chapter 1

Introduction

In this thesis, we research the problem of error propagation in cooperative communication systems. We review previous works done and discuss shortcomings of those works. We then propose a solution to this problem and discuss in detail the merits of the proposed solution.

1.1 Problem Statement

A prominent problem in cooperative systems is the problem of decoding errors at the cooperating terminal (the relay) propagating to the receiving terminal (the destination). Such errors severely degrade the overall performance of the system if not prevented at the relay. Previous work on cooperative communications often assumed that no errors occur at the relay; an assumption that we prove is impractical since even a slight error rate at the relay degrades the overall performance significantly. Other previous research papers have proposed various solutions to overcome the problem of error propagation, which have–to varying degrees– helped to reduce the impact of error propagation.

In this thesis, we investigate an alternative solution to the problem of error propagation in cooperative communication systems and we compare it with previously-proposed solutions.

1.2 Thesis Contributions

Our contributions in this work can be summarized in the following points.

- We propose a novel relaying technique of selectively forwarding bits in a single frame based on the their associated log-likelihood ratios.

- We propose a concatenated coding scheme with iterative decoding to implement the above technique. We note, however, that the proposed technique is not limited to the presented coding scheme, since it is applicable to any coding scheme that can generate LLRs for decoded bits at the relay.

- We analyze the proposed system, where we derive upper bounds on the end-to-end bit error rate that include the most general case of the relay forwarding a subset of the decoded bits, with the possibility of forwarding errors.

- We propose a pragmatic LLR threshold at the relay that relies only on the source-relay channel state. Based on the derived bounds, we optimize this threshold at the relay in terms of the lowest end-to-end bit error rate possible.

- We compare the performance of the proposed technique with that of other previously-mentioned techniques, including forwarding *analog* LLRs (proposed in [1]), with just a CRC check, and with simple DF. We demonstrate via several examples the superiority of the proposed technique.
- Although we analyze the system for only quasi-static source-destination and relay-destination channels, we examine the system for the case in which these channels become more diverse to show the efficacy of our proposed solution in these situations.
- We apply our technique to a cooperative system employing network coding. We investigate both situations of the system not using any channel coding, and a system using the same channel coding scheme proposed in the beginning of the thesis.
- We investigate two schemes for application to network coding. Then, we compare both schemes' performances to establish the better scheme.

1.3 Thesis Outline

The rest of this thesis is organized as follows. Chapter 2 details background information and previous work. Chapter 3 explains in detail the proposed technique for channel-coded cooperative communication systems. Chapter 4 discusses the application of the proposed technique to network-coded cooperative systems (with and without employing channel coding). Finally, Chapter 5 concludes the thesis and provides possible future research directions and improvements.

1.4 Notation

Throughout the rest of the thesis, N will refer to the block length, in bits, of the encoded information frame. We describe the system in a discrete-time baseband-equivalent model, with n as the time index. $\mathcal{Q}(\cdot)$ indicates the Gaussian tail function, and $P(\cdot)$ indicates the probability of an event, while we use $p_Y(y)$ to indicate the probability density function (PDF) of a random variable Y. $E_Y[\cdot]$ indicates expectation with respect to random variable Y, and we use $\bar{Y} = E_Y[y]$ to indicate the mean value. Bold lowercase letters indicate a vector of similarly-named elements, e.g. $\mathbf{b} = [b_1, b_2, \ldots, b_N]$. Finally, $*$ indicates discrete-time convolution, and $\binom{\cdot}{\cdot}$ indicates the binomial coefficient.

Chapter 2

Background

2.1 Cooperative Communications

In an effort to combat fading in wireless channels, methods of exploiting frequency, temporal and spatial diversity have been rigorously studied and applied in several wireless communication standards. Examples of which include frequency diversity combining in wideband code division multiple access (WCDMA), exploiting temporal diversity through channel coding, and most recently spatial diversity combining in wireless fidelity (WiFi, IEEE 802.11n). Spatial diversity, in particular, has been the subject of intense research over the past several years, which is achieved by using multiple antennas to transmit/receive signals over wireless channels, resulting in the so-called multiple-input multiple-output (MIMO) systems. Through different transmit/receive antennas, transmitted signals undergo different fading and hence achieve, when combined, higher diversity [2]. MIMO technology also results in drastic improvements in capacity as compared to single-input single-output systems [3,4].

The down side of MIMO technology, however, is the associated complexity. For instance, for every antenna employed, a separate radio frequency (RF) chain is required, which is bulky and costly. Also, the power consumption is relatively high due to the complex circuitry. Furthermore, the overhead required for training can be significant especially when the underlying channel changes relatively fast. In addition to hardware requirements, antenna spacing requirements also come into play in mobility applications. Namely, multiple antennas on a given terminal must be spaced apart sufficiently to guarantee statistically-independent fading.

In light of these constraints, the MIMO technology is deemed not practical for certain applications where power consumption and/or physical size is an issue. Such applications include cellular networks where it is not practical to mount multiple antennas along with their associated circuitry on a small mobile phone while keeping its size small and its cost affordable. Another example is wireless sensor networks, where the nodes are battery-operated and thus prolonging the battery life as much as possible is a crucial requirement.

An alternate form of obtaining spatial diversity was proposed by many researchers–*cooperative communications* [5–9]. By employing an intermediary relay (or more than one relay) that listens to the source's signal, the relay(s) can then attempt to cooperate with the source by forwarding the message to the destination [5]. Because the destination is getting copies undergoing different fades (by reason of their different points of origin), spatial diversity is achieved at the destination.

Owing to its significant advantages, cooperative communications has emerged recently as a strong candidate for the underlying technology for most future wireless applications, including 4G cellular networks, wireless sensor networks (IEEE 802.15.4), and fixed broadband wireless systems (WiMax, IEEE 802.16j). Among these advantages are 1) the great flexibility in the network configurations whereby the number of cooperating nodes can be changed according to a specified system performance criterion; 2) the relaying strategy can be adapted to fit various scenarios; 3) adaptive modulation and coding can be employed to achieve certain performance objectives; 4) the coverage is expected to be better since users will always find relaying nodes close by even if they are at the far end of their cell; and 5) a consequence of this is an increased user capacity since the user transmitted power can be better controlled which in turn controls the level of multiple access interference at the access point.

Early works on cooperative communications suggested two modes of operation for a cooperating relay [8]: *amplify-and-forward* (AF)–where the relay just amplifies the signal (subject to a power constraint) without decoding it and forwards it to the destination, and *decode-and-forward* (DF)–where the relay detects and demodulates the signal and then re-modulates it and forwards it to the destination. While DF is prone to error propagation due to decoded errors, it simplifies power control at the relay and allows for re-encoding of the signal. AF, however, requires the destination to have full knowledge of the channel state information (CSI) of the source-relay and relay-destination channels, and satisfying the associated power constraint becomes more complicated when the relay lacks CSI knowledge of the source-relay channel. However, AF places the burden of detecting the signal completely on the destination.

More Recently, a few other relaying protocols were proposed. These protocols include *estimate-and-forward* [10, 11] (or EF, an estimate of the transmitted symbol is forwarded to the destination), and *compress-and-forward* [12] (or CF, the estimates are source-coded to exploit possible correlation between channel fades and the source data, then forwarded to the destination). These protocols were shown to improve the end-to-end performance (in terms of capacity [10], received signal-to-noise ratio (SNR) [13], or bit-error rate). However, most of these protocols where analyzed in the case of uncoded transmission, often called *memoryless relaying*–where no channel coding was used at any point in the transmission.

2.2 Challenges in Cooperative Communications

In terms of the end-to-end performance of cooperative communication networks, it has been demonstrated that it significantly depends on the detection reliability at the relay nodes [14]. In the ideal situation where detection at the relays is perfect, the diversity of the system is maintained, that is, as if the relay node is collocated with the transmitting source node [5]. However, with imperfect detection, the diversity degrades. The severity of this degradation depends on the detection reliability level at the relay nodes.

Relays forwarding erroneous bits have an adverse effect on the overall system and, depending on the source-relay channel, can cause an error floor in the end-to-end bit error rate (analogous to a source of interference) [1].

The performance of a cooperative system can be enhanced by using channel coding. Such schemes are usually called *distributed coding* schemes; examples of which include coded cooperation [14–16], and distributed turbo coding (DTC) [1, 17, 18]. Distributed coding schemes have been investigated before, but in a different context. In particular, all coded cooperation schemes have assumed ideal detection at the relay nodes [1, 17], which is idealistic and impractical; since even small error rates at the relay will degrade the diversity gain [18] and might cause an error floor in the end-to-end bit error rate [1]. This motivates us to develop distributed coding schemes under more practical situations.

An additional challenge facing the development of cooperative systems is network throughput, as it is low as compared to that of centralized MIMO systems. This is attributed to the fact that the relay nodes are equipped with single antennas or a small number of antennas, and thus there is no room for achieving any form of multiplexing gains, at least in the conventional sense. In addition, due to some relaying constraints such as half-duplexing, some nodes keep idle while others are relaying, which results in a waste of resources.

2.3 Existing Techniques

2.3.1 Techniques for Mitigating Error Propagation

Relays operating in the DF mode (or a variation thereof) face the problem of decoding errors when the source-relay channel is noisy. For uncoded relaying, the proposed solutions to such a problem can be divided into two types: additional processing at the relay, and additional processing at the destination.

Solutions of the former type include EF [11] (which assumes the relay can output unquantized analog values, and relies on a sign-preserving input-output function that prevents the use of coding), CF [12] (which proves useful if there is an unexploited correlation in the source-relay channel only), constellation re-mapping [19] in case of higher order modulation at the relay (which provides an SNR gain but does not solve the problem of decoding errors), and threshold-DF [20–22] (which decides, on a bit-by-bit basis, whether the relay is active or not based on the source-relay channel energy).

Techniques of the latter type include maximum likelihood (ML) receivers proposed by the authors in [8, 23]. However, both rely on knowing the average bit error rate at the relay, and such an assumption can prove impractical for mobile terminals with fast varying channels.

For the case of channel-coded relaying strategies, previous work often assumed error-free relaying– that the relay can make correct decisions on the bits received and hence is forwarding correct code bits [1, 17]. This assumption is impractical, since even small error rates at the relay will degrade the diversity gain [18] and might cause an error floor in the end-to-end bit error rate [1].

A number of remedies were proposed for relay networks utilizing channel coding. One such technique is using a cyclic redundancy code (CRC) check at the relay [14,15]; preventing it from forwarding if CRC fails. However, a single error in a coded frame would trigger a CRC failure at the relay and hinder a significant number of correct bits to pass on to the destination; resulting in a diversity degradation. Such a problem becomes particularly prominent with larger frame lengths, which is usually the case for distributed coding schemes. Similarly, the authors in [24] proposed that the relay operate in the DF mode when the SNR exceeds a preset value, and in the AF mode below such a value. Such an approach assumes the relay is able to switch between AF and DF modes, and it preempts any re-encoding to happen in case the relay is in the AF mode. Finally, relay selection for coded cooperation was recently proposed by the authors in [16] using a low-complexity metric. However, a sufficient number of relays to choose from is needed to achieve the promised performance improvement.

Alternatively, the authors in [1, 25, 26] proposed to calculate a reliability measure of the received bits and forward that to the destination, which grants the destination additional flexibility in deciding on the bits. While all three papers use the log-likelihood ratio (LLR) as that measure, [1] assumed that the relay can transmit these LLRs as unconstrained analog values to the destination, [25] expanded the rate by transmitting as many as three bits per code bit to relay a quantized value of that measure, and [26] assumed an error-free link between the relay and destination, which can be impractical. Moreover, all three techniques require extra processing at both the relay and destination, and they all complicate diversity combining at the destination since the source and relay will be transmitting different data.

2.3.2 The Use of Network Coding to Increase Throughput

To address the problem of low throughput in cooperative networks, network coding, a coding paradigm initially introduced for routing in computer networks [27–29], has been extended recently to cooperative networks in an effort to enhance their data throughput [30–35]. This is accomplished by allowing multiple data streams arriving from multiple sources to be mixed at intermediate relaying nodes before transmission (see Fig. 2.1 for an example). Consequently, the data transmitted in the network is reduced, resulting in improved throughputs. Not only does network coding improve the network throughput, it also brings other advantages including efficient-energy consumption, network security and network robustness.

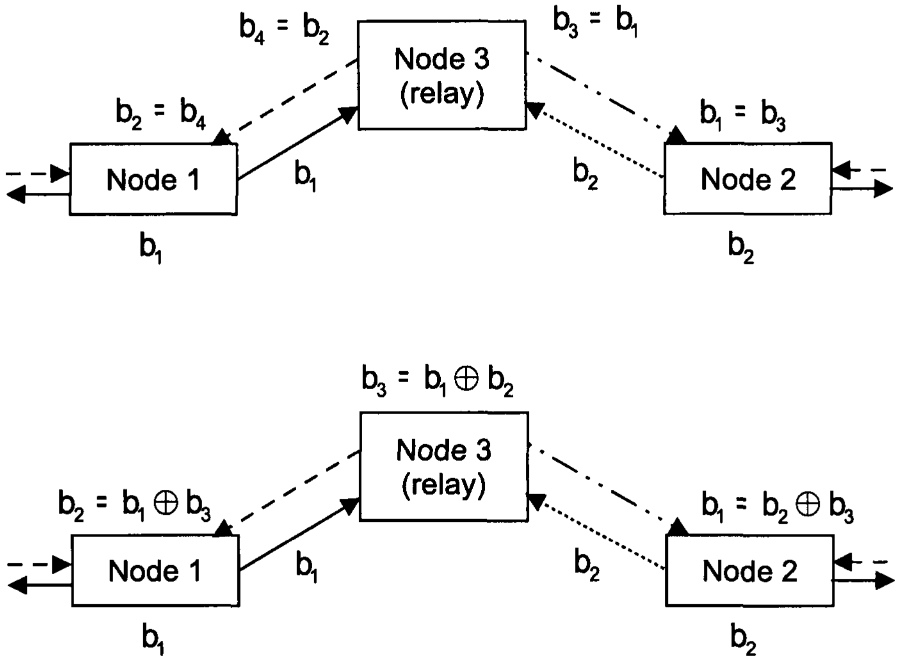

Figure 2.1: An example of how a two-way cooperative system operates without network coding (above) and with network coding (below). Notice that with network coding there was no need to transmit b_4, thus saving throughput

Most of the network coding theory has been applied to wireless networks assuming that the data link layer provides error-free data delivery implying that the underlying error correcting coding scheme is able to correct all errors [31, 32]. However, such an assumption without any error checking schemes (such as ARQ) is impractical as errors will propagate to all terminals and cause diversity loss.

2.4 Conclusions

We have seen in this chapter how there are still serious practical limitations to the full development of cooperative communications. Namely, noisy relays that can propagate decoding errors to the destination. As well as low throughput that results from various constraints applied to relay nodes.

Given the infancy of this research area, we are motivated to believe that further improvements can be made to enhance the error performance of cooperative communications–which we investigate in the next chapter. We are also urged to consider throughput-saving techniques and how to improve their data-link layers–which we discuss in Chapter 4.

Chapter 3

Thresholding to Reduce Error Propagation

In the previous chapter, we have seen how error propagation poses a challenge to cooperative communication systems. As a remedy to the problem of error propagation at relays, we propose to calculate the LLRs of bits received at the relay, and then forwarding only reliable, hard-decided bits to the destination. We propose to distinguish reliable bit from non-reliable ones by means of a threshold. As such, bits with corresponding LLRs that exceed the set threshold are deemed reliable and are forwarded to the destination. Hence, error propagation at the relay is reduced while significant performance improvements are obtained.

In this chapter, we discuss in detail the system model used and the proposed thresholding technique. We derive end-to-end performance analysis and display the potential performance gain in using thresholding in cooperative communication systems. Finally, to validate the claimed improvement, we simulate the system with and without thresholding at the relay and show the comparative advantage of using thresholding.

3.1 Proposed System

The design of the system presented here aims at enabling the use of our technique in a coded cooperative scenario. In our system, the source encodes N information bits using a rate 1/4 serially-concatenated convolutional code (SCCC), with two recursive systematic convolutional (RSC) codes (each with rate 1/2) as constituent encoders (denoted by E_1 and E_2 for the outer and inner encoders, respectively). As shown in the source block in Fig. 3.1, let $\mathbf{b} = [b_1, \ldots, b_N]$ be the frame of information bits to be encoded, and $\mathbf{p} = [p_1, \ldots, p_N]$ be the parity bits added by E_1. Hence $\mathbf{c} = [c_1, \ldots, c_{2N}] = [b_1, p_1 \ldots, b_N, p_N]$ will be the output of E_1. As shown in the diagram, $\mathbf{u} = \Pi(\mathbf{c})$ or the interleaved $\mathbf{c}$, which is the input to E_2. Similarly, let $\mathbf{w} = [w_1, \ldots, w_{2N}]$ be the parity bits added by E_2. Hence, the output of E_2 is $\mathbf{x} = [x_1, \ldots, x_{4N}] = [u_1, w_1, \ldots, u_{2N}, w_{2N}]$. For the rest of this work, we assume a single cooperating relay and binary phase shift keying (BPSK) modulation throughout, although the technique is expandable to higher-order modulation with multiple relays (an example would be nulling the symbol if any of the constituent bits are nulled). For notational expedience, we assume that the bits take values $\in \{\pm 1\}$. Finally, we assume throughout the thesis that all receiving nodes have perfect knowledge of channel state information (CSI).

We stress here that although we present the proposed technique in the context of this system, it is applicable to other coding strategies as well; given that LLR values can be obtained of the relay output. See Fig.3.1 for a block diagram of the proposed system.

3.1.1 Overview

Observing that $\mathbf{u}$ is a part of $\mathbf{x}$, and that $\mathbf{u}$ can be obtained by decoding $\mathbf{x}$, we exploit this structure by letting the source broadcast $\mathbf{x}$ in the first stage, then transmit $\mathbf{u}$ in the second stage. After the relay listens to the source in the first stage, it can decode $\mathbf{x}$ to obtain $\mathbf{u}$ and cooperate with the source in the second stage. We note that this decreases the overall system code rate since $\mathbf{u}$ is transmitted twice, first as a part of $\mathbf{x}$ and then alone. To obtain a higher code rate, we can reduce the number of repeated bits by puncturing a part of $\mathbf{u}$ out of $\mathbf{x}$ during the first stage.

Hence, the overall code rate can be split into equivalent code rates for both stages, namely R_{c_1} and R_{c_2}, where R_{c_1} ranges from 1/4 (transmitting $\mathbf{x}$ in full) to 1/2 (puncturing all of $\mathbf{u}$ out of $\mathbf{x}$), and $R_{c_2} = 1/2$. Consecutively, the overall system code rate will be equal to $\frac{1}{(1/R_{c_1})+(1/R_{c_2})}$. The timeline for the transmission of a single frame of information is thus $n = 1, 2, \ldots, N/R_{c_1}$ (broadcast stage), and

$n = N/R_{c_1} + 1, \ldots, \left(\frac{1}{R_{c_1}} + \frac{1}{R_{c_2}}\right) N$ (cooperation stage).

3.1.2 The Broadcast Stage

We elect to use $R_{c_1} = 1/3$, which is obtained by puncturing half of $\mathbf{u}$ out of $\mathbf{x}$. Hence the modulated output of the source can be expressed as $\{y[n]\} = \{w_1, u_2, w_2, w_3, u_4, w_4, \ldots\}$ and so on. During this stage, the signals received at the destination and the cooperating relay can be expressed as

$$r_{SD}[n] = \sqrt{R_{c_1} E_b} h_{SD}[n] y[n] + n_{SD}[n], \tag{3.1}$$

$$r_{SR}[n] = \sqrt{R_{c_1} E_b} h_{SR}[n] y[n] + n_{SR}[n], \tag{3.2}$$

respectively, where $n = 1, 2, \ldots, N/R_{c_1}$, $h_{SD}[n]$ and $h_{SR}[n]$ are the fading coefficients for the source-destination and source-relay channels, respectively, and E_b is the energy transmitted per bit from the source. n_{SD} and n_{SR} are complex additive white Gaussian noise (AWGN) signals with variance $N_0/2$ per dimension.

After the relay receives r_{SR}, a SISO decoder is used (shown in Fig. 3.1 as D_2, here an *a posteriori* probability (APP) decoder) which is matched to E_2 to obtain soft estimates of $\mathbf{u}$, denoted by $\Lambda_{\mathbf{u}}$.[1] Specifically, these soft estimates are LLRs, formally defined as

$$\Lambda_{u_i} = \log_e \frac{P\left(u_i = 1 | h_{SR}, r_{SR}\right)}{P\left(u_i = -1 | h_{SR}, r_{SR}\right)}, \tag{3.3}$$

[1]One can also use a soft-output Viterbi algorithm (SOVA) to produce these soft estimates [36]

which are used as reliability measures of the individual bits.

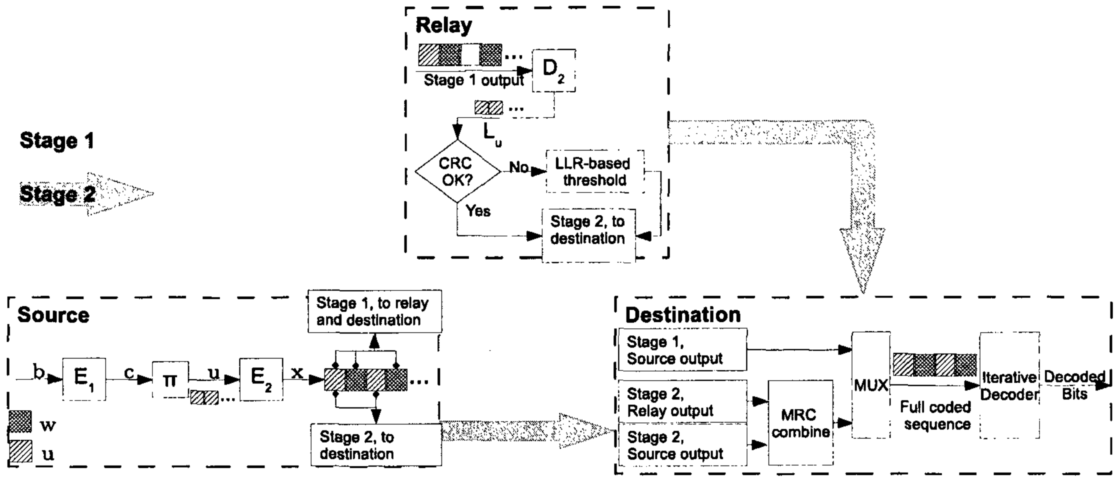

Figure 3.1: System block diagram, E_1, E_2 are the constituent encoders, D_2 is an APP decoder matched to E_2, and Π is an interleaver

3.1.3 The Cooperation Stage

In this stage, the source transmits $\mathbf{u}$ to the destination, while the relay cooperates with the source by sending the same data. Observing that the relay has, from the previous stage, the set of soft information $\Lambda_{\mathbf{u}}$, it can use this information in several ways. The relay can either: forward hard decisions based on the sign of the soft estimates (we refer to this case as simple DF for the rest of this work), or employ a scheme to reduce error propagation to the destination. From the previous schemes discussed earlier, we focus on using a CRC check (discarding the frame if CRC failed, cf. [15]), and forwarding analog LLRs (after normalizing their power, as described in [1]). Our proposed technique, however, is to set a threshold T at the relay. Then, only bits that have associated LLRs exceeding T, in absolute value, will be forwarded.

The relay then keeps silent (transmits zero energy) in place of the blocked bits.[2] To prevent correct bits from being blocked, we set the threshold to operate only after a CRC check fails, such that no bits are blocked when we know the frame has been successfully decoded. During this stage, we can express the signals received at the destination from the relay and source as

$$r_{RD}[n] = \sqrt{R_{c2}\frac{E_b}{2}} h_{RD}[n]\hat{u}[n] + n_{RD}[n], \tag{3.4}$$

$$r_{SD}[n] = \sqrt{R_{c2}\frac{E_b}{2}} h_{SD}[n]u[n] + n_{SD}[n], \tag{3.5}$$

respectively, where $n = N/R_{c_1}1, \ldots, \left(\frac{1}{R_{c_1}} + \frac{1}{R_{c_2}}\right)N$, and $\hat{u}[n]$ and $u[n]$ are the modulated output of the relay and source, respectively. Other variable definitions are similar to those found in (3.1) and (3.2). We divide E_b by 2 to maintain a constant energy per bit across the two stages.

3.1.4 Decoding at the Destination

The destination receives both the broadcast stage frame (3.1), and the cooperation stage frames (3.4), (3.5). The destination combines the two copies of the cooperation stage frame using maximum ratio combining (MRC), then multiplexes the combined frame with the broadcast stage frame to get the complete coded frame. An iterative decoder, as described in [37, p.174], decodes the frame and produces the information bits. We summarize the operation of our proposed system in Fig. 3.1. Consequently,

[2]For reason of tractability of the analysis, we assume the relay does not allocate the energy of the blocked bits to the forwarded ones; effectively lowering the total transmit power.

using such a setup will increase the overall system code rate to $\frac{1}{(1/R_{c_1})+(1/R_{c_2})} = 1/5$. Of course, further puncturing can be used to achieve higher code rates.

3.2 Performance Analysis

To analyze the performance of our system, we derive union bounds on the end-to-end bit error rate. We also assume Rayleigh-faded channels throughout.

3.2.1 Relayed Frame Includes Nulled and Error Bits

During the first stage, the destination only receives r_{SD} expressed in (3.1). Hence, the receive-SNR can be expressed as

$$\gamma_{D_1}[n] = 2\frac{R_{c_1}E_b}{N_0}\left|h_{SD}[n]\right|^2 : n = 1, 2, \ldots, N/R_{c_1}.$$

During the second stage, the destination receives r_{RD} and r_{SD} expressed in (3.4) and (3.5), respectively. The destination then combines both signals using an MRC combiner. Thus, the output of the MRC combiner can be expressed as

$$\begin{aligned} r_{\mathrm{MRC}}[n] &= h^*_{SD}[n]r_{SD}[n] + h^*_{RD}[n]r_{RD}[n] \\ &= h^*_{SD}[n]\left(\sqrt{R_{c_2}\frac{E_b}{2}}h_{SD}[n]u[n] + n_{SD}[n]\right) \\ &\quad + h^*_{RD}[n]\left(\sqrt{R_{c_2}\frac{E_b}{2}}h_{RD}[n]\hat{u}[n] + n_{RD}[n]\right). \end{aligned} \tag{3.6}$$

To combine $u[n]$ and $\hat{u}[n]$, we define $A[n]$ to distinguish a wrong decoded bit from a correct one, formally defined as

$$A[n] \triangleq \begin{cases} +1, & u[n] = \hat{u}[n] \\ -1, & u[n] \neq \hat{u}[n], \hat{u}[n] \neq 0, \\ 0, & \hat{u}[n] = 0. \end{cases}$$

Thus, $\hat{u}[n] = A[n]u[n]$, and (3.6) simplifies to

$$\begin{aligned} r_{\mathrm{MRC}}[n] = &\left(|h_{SD}[n]|^2 + A[n]\,|h_{RD}[n]|^2\right)\left(\sqrt{R_{c_2}\frac{E_b}{2}}h_{SD}[n]u[n]\right) \\ &+ \left(h^*_{SD}[n]n_{SD}[n] + h^*_{RD}[n]n_{RD}[n]\right). \end{aligned} \tag{3.7}$$

Hence, the receive-SNR for the second stage can be expressed as

$$\gamma_{D_2}[n] = \frac{R_{c_2}E_b}{N_0}\frac{\left(|h_{SD}[n]|^2 + A[n]\,|h_{RD}[n]|^2\right)^2}{\left(|h_{SD}[n]|^2 + |h_{RD}[n]|^2\right)} : n = N/R_{c_1} + 1, \dots, \left(\frac{1}{R_{c_1}} + \frac{1}{R_{c_2}}\right)N.$$

Finally, the total receive-SNR at the output of the multiplexer can be expressed as

$$\gamma_D[n] = \begin{cases} 2R_{c_1}\gamma_{SD}[n], & n = 1, 2, \dots, N/R_{c_1}, \\ R_{c_2}\frac{(\gamma_{SD}[n] + A[n]\gamma_{RD}[n])^2}{(\gamma_{SD}[n] + \gamma_{RD}[n])}, & n = N/R_{c_1} + 1, \dots, \left(\frac{1}{R_{c_1}} + \frac{1}{R_{c_2}}\right)N, \end{cases} \tag{3.8}$$

where $\gamma_{SD}[n] = \frac{E_b}{N_0}|h_{SD}[n]|^2, \gamma_{RD}[n] = \frac{E_b}{N_0}|h_{RD}[n]|^2$. Hence, assuming the all-zero codeword was transmitted, the probability of the destination erroneously decoding a codeword of weight d bits (also called the pairwise error probability, or PEP) conditioned over the instantaneous SNRs $\gamma_{SD}[n], \gamma_{RD}[n]$, can be found as

$$P\left(d|\gamma_{SD}[n], \gamma_{RD}[n]\right) = \mathcal{Q}\left(\sqrt{\sum_{n=i}^{i+d-1} \mp\gamma_{D}[n]}\right) \qquad \forall i \in 0, \ldots, 4N-d, \tag{3.9}$$

where $\mp$ stands for the case of $A[n] = -1$ with $\gamma_{SD}[n] < \gamma_{RD}[n]$ and otherwise, respectively. To proceed with the analysis further, we assume that the source-destination and relay-destination channels exhibit quasi-static fading (the whole frame sees the same fade) , whereas the source-relay channel is block faded. We acknowledge that this channel model is limited from a practical point of view. However, we adopt it because it makes the analysis more tractable, which otherwise becomes prohibitively complex due to the multidimensional integrations involved. We use these results as proof of concept. Nevertheless, we provide simulation results for various practical channels models to domesticate the efficacy of the proposed scheme. Consequently, $\gamma_{SD}[n] = \gamma_{SD}, \gamma_{RD}[n] = \gamma_{RD}$.

Since the coded frame is received over two stages, we split d into $d_1 + d_2 = d$, where d_1 and d_2 refer to the weight of the error event during the first and second stages, respectively. We split d_2 to account for the possibility of having bits nulled at the relay into $d_2 = d_r + d_\phi$, where d_r indicates the weight of bits (in the error event) receiving contribution from the relay during the second stage, and d_ϕ equals to the number of bits receiving contribution from the source only during the second stage.

Since the relay can forward wrong bits, we further split $d_r = d_c + d_e$, where d_c and d_e equal to the number of bits correctly and wrongly relayed from the relay in the error event, respectively. For notational expedience, we define ξ_1 and ξ_2 as

$$\xi_1 \triangleq 2d_1 R_{c_1}\gamma_{SD} + d_c R_{c_2}\left(\gamma_{SD} + \gamma_{RD}\right) + d_e R_{c_2}\frac{\left(\gamma_{SD} - \gamma_{RD}\right)^2}{\gamma_{SD} + \gamma_{RD}} + d_\phi R_{c_2}\frac{\gamma_{SD}^2}{\gamma_{SD} + \gamma_{RD}},$$

and

$$\xi_2 \triangleq 2d_1 R_{c_1}\gamma_{SD} + d_c R_{c_2}\left(\gamma_{SD} + \gamma_{RD}\right) - d_e R_{c_2}\frac{\left(\gamma_{SD} - \gamma_{RD}\right)^2}{\gamma_{SD} + \gamma_{RD}} + d_\phi R_{c_2}\frac{\gamma_{SD}^2}{\gamma_{SD} + \gamma_{RD}},$$

respectively, where the negative sign in ξ_2 was used to account for the negative amplitude of the signal component in r_{MRC} in (3.7). Hence, for the case of $\gamma_{SD} \geq \gamma_{RD}$, the expression in (3.9) can be expanded as

$$P\left(d|d_c, d_e, d_\phi, \gamma_{SD}, \gamma_{RD} : \gamma_{SD} \geq \gamma_{RD}\right) = \mathcal{Q}\left(\sqrt{\xi_1}\right). \tag{3.10}$$

[3]However, for the case where $\gamma_{SD} < \gamma_{RD}$ and $\xi_2 \geq 0$, (3.9) can be expanded as

$$P\left(d|d_c, d_e, d_\phi, \gamma_{SD}, \gamma_{RD} : \gamma_{SD} < \gamma_{RD}, \xi_2 \geq 0\right) = \mathcal{Q}\left(\sqrt{\xi_2}\right), \tag{3.11}$$

[3]It is important to note here that we do not assume that the destination knows the locations of blocked bits; which is evident from having γ_{RD} in the denominator of the coefficient of d_ϕ

while for the case of $\xi_2 < 0$, the expression in (3.9) becomes

$$P\left(d|d_c, d_e, d_\phi, \gamma_{SD}, \gamma_{RD} : \gamma_{SD} < \gamma_{RD}, \xi_2 < 0\right) = 1 - \mathcal{Q}\left(\sqrt{-\xi_2}\right). \tag{3.12}$$

To obtain the PEP conditioned only on (d_c, d_e, d_ϕ), we integrate (3.9) over the joint PDF of $(\gamma_{SD}, \gamma_{RD})$. Assuming that the fades experienced by the source-destination and relay-destination channels are independent, and given that γ_{SD}, γ_{RD} have an exponential distribution (taking the general form $p_\gamma(\gamma) = \frac{1}{\bar{\gamma}}\exp\left(-\frac{\gamma}{\bar{\gamma}}\right)$), the PEP becomes

$$\begin{aligned}
&P\left(d|d_c, d_e, d_\phi\right) = \\
&\iint_{\gamma_{SD}\geq\gamma_{RD}} \mathcal{Q}\left(\sqrt{2d_1 R_{c_1}\gamma_{SD} + d_c R_{c_2}\left(\gamma_{SD}+\gamma_{RD}\right) + d_e R_{c_2}\frac{\left(\gamma_{SD}-\gamma_{RD}\right)^2}{\gamma_{SD}+\gamma_{RD}} + d_\phi R_{c_2}\frac{\gamma_{SD}^2}{\gamma_{SD}+\gamma_{RD}}}\right) \\
&\cdot\left(\frac{1}{\bar{\gamma}_{SD}\bar{\gamma}_{RD}}\right)\exp\left(\frac{\gamma_{SD}}{\bar{\gamma}_{SD}}\right)\exp\left(\frac{\gamma_{RD}}{\bar{\gamma}_{RD}}\right)d\gamma_{SD}d\gamma_{RD} \\
&+\iint_{\gamma_{SD}<\gamma_{RD},\xi_2\geq 0} \mathcal{Q}\left(\sqrt{\xi_2}\right)\left(\frac{1}{\bar{\gamma}_{SD}\bar{\gamma}_{RD}}\right)\exp\left(\frac{\gamma_{SD}}{\bar{\gamma}_{SD}}\right)\exp\left(\frac{\gamma_{RD}}{\bar{\gamma}_{RD}}\right)d\gamma_{SD}d\gamma_{RD} \\
&+\iint_{\gamma_{SD}<\gamma_{RD},\xi_2<0}\left[1-\mathcal{Q}\left(\sqrt{-\xi_2}\right)\right]\left(\frac{1}{\bar{\gamma}_{SD}\bar{\gamma}_{RD}}\right)\exp\left(\frac{\gamma_{SD}}{\bar{\gamma}_{SD}}\right)\exp\left(\frac{\gamma_{RD}}{\bar{\gamma}_{RD}}\right)d\gamma_{SD}d\gamma_{RD},
\end{aligned} \tag{3.13}$$

where $\bar{\gamma}_{SD} = \frac{E_b}{N_0}E_{H_{SD}}\left[|h_{SD}|^2\right], \bar{\gamma}_{RD} = \frac{E_b}{N_0}E_{H_{RD}}\left[|h_{RD}|^2\right]$. We note from (3.13) that in all cases where $d_e > 0$ the resultant PEP will increase. Note that the PEP expression given in (3.13) is conditional on d_e, d_c, d_ϕ (or $d_e, d_r : d_r = d_c + d_e, d_r = d_2 - d_\phi$) which are specific to a group of error events of weight d. Thus, we need to sum the PEP over the probability of an error word of weight d having d_r and d_e as components.

That is,

$$P(d) = \sum_{d_r=0}^{d_2} \sum_{d_e=0}^{d_r} P(d|d_e, d_r) p_{d_e}(d_e) p_{d_r}(d_r). \tag{3.14}$$

Assuming a uniform distribution of relayed and error bits over the forwarded frame,[4] the PDF functions for d_r and d_e are equal to

$$p_{d_r}(d_r) = \frac{\binom{d_2}{d_r}\binom{2N-d_2}{d_R-d_r}}{\binom{2N}{d_R}}, \quad p_{d_e}(d_e) = \frac{\binom{d_r}{d_e}\binom{d_R-d_r}{d_E-d_e}}{\binom{d_R}{d_E}}, \tag{3.15}$$

respectively, where d_R and d_E represent the total number of forwarded bits from the relay and the number of which are wrong, respectively. Finally, assuming ML decoding of the received codeword at the destination, the resultant bit error rate can be upper-bounded by (cf. [38])

$$P_b(e) < \sum_{d=d_{\text{free}}}^{\infty} \sum_{i=1}^{N} \frac{i}{N} \binom{N}{i} p(d|i) P(d), \tag{3.16}$$

where d_{free} is the free Hamming distance of the SCCC and $p(d|i)$ is the input/output weight distribution function of the SCCC code.

A closed-form solution for (3.13) requires the evaluation of an integral of the form $\int_0^\infty \exp(-c_1 u - c_2/u) du$. Furthermore, the integration regions of $\xi_2 < 0, \xi_2 \geq 0$ are quadratic functions of $(\gamma_{SD}, \gamma_{RD})$. Due to the complexity of such an expression, we opt to evaluate (3.13) using numerical integration.

[4] We note that the actual distribution of error/relayed bits' positions might not be uniform, since particular error events are more probable than others. However, we use this assumption to simplify the analysis, and we demonstrate later that there is an agreement between theory and simulations.

Next, we evaluate the obtained expression for the PEP under two assumptions, for the purpose of further validating the PEP.

3.2.2 Relayed Frame Includes Nulled but no Error Bits

In partial error-free cooperation, we assume two assumption: that the relay only forwards a portion of the decoded bits, and that the forwarded bits are all correct. In light of the previous analysis, d_E is in this case always zero, but $d_R \in \{0, \ldots, 2N\}$ bits. Hence, $p_{d_e}(d_e) = 1$ for $d_e = 0$. Consequently, the expression of the conditional PEP in (3.13) becomes

$$\begin{aligned} &P\left(d|d_c, d_\phi\right) = \\ &\int_0^\infty \int_0^\infty \mathcal{Q}\left(\sqrt{2d_1 R_{c_1}\gamma_{SD} + d_c R_{c_2}\left(\gamma_{SD}+\gamma_{RD}\right) + d_\phi R_{c_2}\frac{\gamma_{SD}^2}{\gamma_{SD}+\gamma_{RD}}}\right) \\ &\cdot \left(\frac{1}{\bar{\gamma}_{SD}\bar{\gamma}_{RD}}\right) \exp\left(\frac{\gamma_{SD}}{\bar{\gamma}_{SD}}\right) \exp\left(\frac{\gamma_{RD}}{\bar{\gamma}_{RD}}\right) d\gamma_{SD} d\gamma_{RD}. \end{aligned} \tag{3.17}$$

The average PEP is again obtained by averaging over $p_{d_r}(d_r)$

$$P(d) = \sum_{d_r=0}^{d_2} P(d|d_c = d_r) p_{d_r}(d_r),$$

where $p_{d_r}(d_r)$ has the same definition in (3.15). Thus, we can see this assumption eliminates the error floor from the PEP and bit error rate. However, there will still be a loss of diversity due to the possibility of error events that have $d_c = 0, (d_\phi + d_1) <$

d_{free}. Such loss of diversity can be witnessed when the relay is able to block all errors from passing to the destination, but nulls correct bits in the process of doing so.

3.2.3 Ideal Relaying

We include this case for mathematical completeness, despite having no practical application. Assuming the relay is able to forward all bits correctly, rendering $d_R = 2N = d_C, d_E = 0$, and thus both $p(d_r) = 1$ when $d_r = d_R = 2N, p(d_e) = 1$ when $d_e = 0$. The average PEP in (3.17) evaluates to

$$P(d) = \int_0^\infty \int_0^\infty Q\left(\sqrt{2d_1 R_{c_1}\gamma_{SD} + d_2 R_{c_2}\left(\gamma_{SD} + \gamma_{RD}\right)}\right)$$

$$\cdot \left(\frac{1}{\bar{\gamma}_{SD}\bar{\gamma}_{RD}}\right) \exp\left(\frac{\gamma_{SD}}{\bar{\gamma}_{SD}}\right) \exp\left(\frac{\gamma_{RD}}{\bar{\gamma}_{RD}}\right) d\gamma_{SD} d\gamma_{RD}.$$

The expression above evaluates to, using Craig's formula (cf. [39])for the Q-function and assuming $\bar{\gamma}_{SD} = \bar{\gamma}_{RD}$,

$$P(d) = \frac{1}{\pi}\int_0^{\pi/2} \left(\frac{1}{1+s_1\bar{\gamma}}\right)\left(\frac{1}{1+s_2\bar{\gamma}}\right) d\theta, \tag{3.18}$$

where $s_1 = \frac{2d_1 R_{c_1} + d_2 R_{c_2}}{2\sin^2\theta}$ and $s_2 = \frac{d_2 R_{c_2}}{2\sin^2\theta}$. To see the diversity order of the PEP (and consequently the resulting bit error rate), we can simplify (3.18) by assuming $(2R_{c_1}d_1 + R_{c_2}d_2)\bar{\gamma} \gg 2$. The expression of the PEP thus tends to

$$P(d) \approx \frac{3}{\left(4R_{c_2}d_2\right)\left(R_{c_1}d_1 + \frac{R_{c2}}{2}d_2\right)\left(\bar{\gamma}\right)^2},$$

which suggests a diversity order of two.

3.3 Optimizing the Threshold at the Relay

We can see from (3.13)-(3.18) that the best performance (ignoring any other restrictions) would be at $d_E = 0, d_R = 2N$ (achieves full diversity and no error floor). However, the possible combinations of these two values are restricted by the system employed. Generally speaking, decreasing d_E (by means of a stricter threshold) would also decrease d_R, and vice versa. We next study two thresholding schemes: The first is a genie-aided threshold that relies on knowing the positions of the errors, and the second is a practical threshold relying only on the knowledge of CSI (of the source-relay channel). We discuss optimizing both thresholds to achieve the minimum end-to-end bit error rate.

3.3.1 Genie-Aided Threshold

As a *benchmark* for any thresholding scheme, we assume that for any given frame the relay knows the location of errors. Although impractical, this assumption provides us with a limiting case for more practical thresholding schemes. Given that the relay knows the LLR values of all wrong bits, a threshold can be set as the absolute value of any of these LLRs; preventing all but the desired number of errors to be forwarded. Let Λ_{wrong} be the set of bits that are known to be wrong, formally defined as $\Lambda_{\text{wrong}} = \{|\Lambda_u[n]|\}_{n:\text{sign}(\Lambda_u[n]) \neq u[n]}$. Assuming Λ_{wrong} is sorted in a decreasing order, we then formally define genie-aided thresholds as

$$T_0 = \Lambda_{\text{wrong}_1}, T_1 = \Lambda_{\text{wrong}_2}, T_2 = \Lambda_{\text{wrong}_3}, \ldots, \tag{3.19}$$

where T indicates the value of the LLR threshold, and the sub-index indicates the number of errors allowed to pass. The question of optimality here is to choose the threshold that results in the minimum end-to-end bit error rate; keeping in mind that allowing a few errors to pass also allows correct bits that can contribute to the overall performance.

The mathematical analysis of this case is beyond the scope of this work, by reason of its impracticality. We nevertheless provide simulation results (displayed in Fig. 3.2) that illustrate that the optimal choice in this case would be allowing no errors to pass at all, especially at higher SNR values.

3.3.2 Proposed (CSI-Based) Threshold

Observing that the instantaneous PDF of the LLR values at the relay depends on the underlying source-relay CSI. We propose a metric that relies only on the CSI of the source-relay channel.

Denoted by Z, this metric is equal to the mean source-relay channel energy during the transmission of the current frame, formally defined as

$$Z \triangleq \frac{R_{c_1}}{N} \sum_{n=1}^{N/R_{c_1}} |h_{SR}[n]|^2 .$$

We can then set a threshold that is proportional to Z as,

$$T_Z = \alpha Z + \beta. \tag{3.20}$$

Theorem 1. *Such a threshold approximates a constant source-relay bit error rate.*

Proof. For a SISO decoder, the LLRs can be approximated (especially at high input SNR) to follow a normal distribution, with $\gamma_{r,out} \leq Rd_{free}\gamma_{r,in} = Rd_{free}\frac{E_b|h|^2}{N_0}$ (cf. [1]). If we set a threshold T over the LLRs, then for any two instances of h, e.g. $h_1, h_2 : |h_2| > |h_1|$, the conditional bit error rate will hence be (given that $u = -1$)

$$P(L_u(h_1) > T(h_1)) \text{ and } P(L_u(h_2) > T(h_2)),$$

respectively. By equating both probabilities, we obtain

$$P(L_u(h_1) > T(h_1)) = P(L_u(h_2) > T(h_2)) \Rightarrow Rd_{free}\frac{E_b|h_2|^2}{N_0} - Rd_{free}\frac{E_b|h_1|^2}{N_0} = T(h_2) - T(h_1).$$

Assuming $T(h) = \alpha|h|^2 + \beta \Rightarrow Rd_{free}\frac{E_b}{N_0}\left(|h_2|^2 - |h_1|^2\right) = \alpha\left(|h_2|^2 - |h_1|^2\right)$. Hence, setting $\alpha = Rd_{free}\frac{E_b}{N_0}$ and an arbitrary β guarantees a constant bit error rate across different channel realizations. $\square$

We can then model the resultant (d_E, d_C) as jointly independent binomial random variables. As such, the resultant PEP at the destination is expressed as

$$P(d) = \sum_{d_R=0}^{N/R_{c2}} \sum_{d_E=0}^{d_R} \sum_{d_r=0}^{d_2} \sum_{d_e=0}^{d_r} \left[P(d|d_e, d_r = d_c + d_e) p_{d_e}(d_e|d_E, d_R) p_{d_r}(d_r|d_R) p_{d_E}(d_E) p_{d_R}(d_R) \right], \tag{3.21}$$

where the underlying PDFs are defined as,

$$p_{d_r}(d_r|d_R) = \frac{\binom{d_2}{d_r}\binom{2N-d_2}{d_R-d_r}}{\binom{2N}{d_R}}, \quad p_{d_e}(d_e|d_R, d_E) = \frac{\binom{d_r}{d_e}\binom{d_R-d_r}{d_E-d_e}}{\binom{d_R}{d_E}},$$
$$p_{d_E}(d_E) = \mathcal{B}\left(d_E, N/R_{c_2}, \frac{\bar{d}_E}{N/R_{c_2}}\right), \quad p_{d_C}(d_C) = \mathcal{B}\left(d_C, N/R_{c_2}, \frac{\bar{d}_C}{N/R_{c_2}}\right)$$
$$p_{d_R}(d_R = d_C + d_E) = p_{d_C}(d_C) * p_{d_E}(d_E),$$

where $\mathcal{B}(x, k, p)$ indicates the binomial distribution with k and p as the number of trials and the probability of success, respectively. The last step in deriving the optimal CSI-based threshold is establishing the relationship between T_Z and $\left(\bar{d}_E, \bar{d}_R\right)$. Since such a relationship will depend on the code used between the source and relay and the type of decoder used at the relay, we opt to find this relationship empirically. Consequently, we select the $\left(\bar{d}_E, \bar{d}_R\right)$ pair that minimizes the end-to-end bit error rate in (3.16) when the corresponding $P(d)$ found in (3.21) is used. We point out that since we are relying on an upper-bounded bit error rate expression to optimize the threshold, we choose the threshold based on the SNR region in which the upper bound converges to the actual performance, namely, the region of high SNR.

Table 3.1: SCCC weight distribution function, $M(d,i)$ refers to the number of codewords of weight d resulting from an input of weight i, $p(d|i) = \frac{M(d,i)}{\binom{N}{i}}$

d	$M(d,i=1)$	$M(d,i=2)$	$M(d,i=3)$	$M(d,i=4)$
3	1	0	0	0
4	1	0	0	0
5	0	1	0	0
6	1	0	0	0
7	0	2	1	0
8	1	3	2	0
9	0	0	3	1
10	1	3	3	0
11	0	1	5	5
12	1	4	3	7
13	1	5	9	10
14	0	1	11	11
15	1	5	14	20
16	1	97	14	22
17	0	5	19	34
18	1	3	20	223
19	0	4	118	52
20	1	7	122	150
21	0	2	32	188
22	1	7	123	90
23	0	4	34	302
24	1	8	122	498
25	1	11	48	179
26	0	5	129	521
27	1	10	63	323
28	1	95	153	1001
29	0	7	155	731
30	1	6	75	957

3.4 Simulation Results and Discussion

The system used in the simulations is depicted in Fig. 3.1. Throughout our simulations, the system encodes a frame of $N = 100$ information bits, with $R_{c_1} = 1/3$ and $R_{c_2} = 1/2$. The constituent codes of the SCCC, for all simulated schemes, were $(13, 17)_8$ for the outer code, $(27, 31)_8$ for the inner code (see Table 3.1 for the obtained weight-distribution function), and the iterative decoder was set to run for 5 iterations. The assumed source-relay channel is block-faded with 20 independently-faded blocks and $\bar{\gamma}_{SR}$ taking values from $\{6, 9\}$ dB, as well as quasi-static source-destination and relay-destination channels.[5]

3.4.1 Optimizing the Threshold

In light of the discussion in Section 3.3, we find the best thresholds of the two cases where the relay knows error positions (genie-aided) and using the CSI-based threshold.

Optimal Genie-Aided Threshold

Assuming that we are able to strictly control d_E, we explore under various $\bar{\gamma}_{SR}$ values the optimal threshold to set at the relay. The end-to-end performance is demonstrated in Fig. 3.2, where we can see the performance of different genie-aided thresholds under various SNR values. For both $\bar{\gamma}_{SR}$ values, we can see that the best performance is obtained when the threshold prevents all errors from passing. On the other hand,

[5]We emphasize here again that this particular combination of channel models is of limited practicality. However, we use it as a proof-of-concept and to facilitate optimizing the threshold.

we see that allowing 1 or 2 errors to pass (denoted by T_1, T_2, respectively) does not provide any noticeable gain, even at low values of $\bar{\gamma}$. By increasing $\bar{\gamma}_{SR}$ from 6 to 9 dB, the source-relay bit error rate decreases, resulting in higher diversity for T_0 and a lower error floor in the end-to-end bit error rate for T_1, T_2. We conclude from these results that for a genie-aided threshold, the best performance is achieved by preventing all errors from passing to the destination *regardless of the source-relay average SNR.*

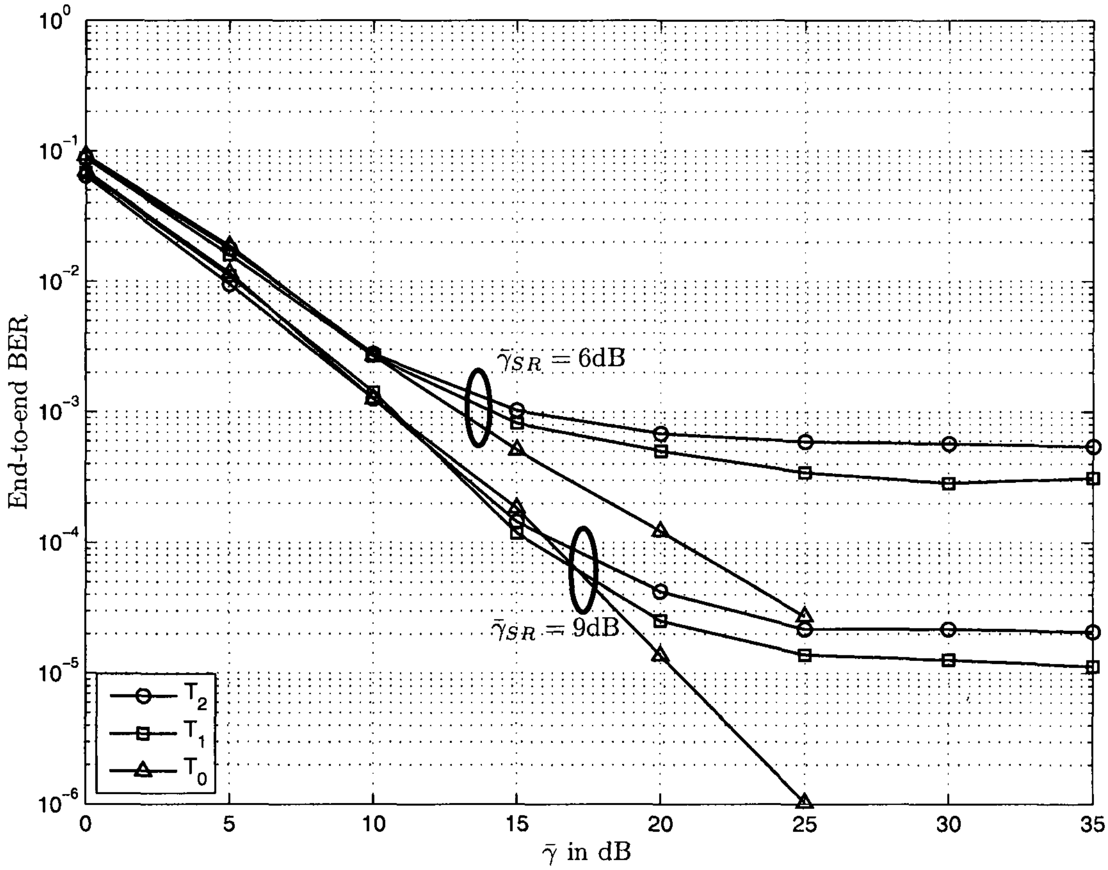

Figure 3.2: End-to-end bit error rate vs. $\bar{\gamma}$ for genie-aided thresholds T_0, T_1, T_2

Optimal CSI-Based Threshold

We simulate the source-relay part of the system under different values of $\bar{\gamma}_{SR}$, α and β in (3.20) to obtain the possible $\left(\bar{d}_E, \bar{d}_C\right)$ operation values. In Fig. 3.3 we plot the obtained possible values. We can see that in general a higher $\bar{\gamma}_{SR}$ value allows for better selectability of the threshold (i.e. allowing fewer errors while blocking less correct bits). Moreover, we can see that increasing α and β results generally in a stricter threshold; allowing less errors but blocking more correct bits. By substituting these possible pairs in the PEP expression in (3.21), and then in the end-to-end bit error rate expression in (3.16) (evaluated only at $\bar{\gamma} = 30$ dB,) we obtain Fig. 3.4, where the end-to-end bit error rate is shown versus possible combinations of α, β. We can see a region of minimum bit error rate on both surfaces. The optimal point of operation for both values of $\bar{\gamma}_{SR} = 6, 9$ dB were found to be $\alpha = 0.5, \beta = 2.5$ for $\bar{\gamma}_{SR} = 6$ dB, and $\alpha = 0.5, \beta = 2.0$ for $\bar{\gamma}_{SR} = 9$ dB.

3.4.2 Thresholding vs. Other Error Control Techniques at the Relay

To illustrate the strength of our proposed system, we simulate other protocols at the relay. Namely, employing only a CRC check at the relay (thus discarding frames that fail that check), forwarding analog LLR values (cf. [1]), and simple DF, while also displaying the performance of the optimized thresholds obtained previously (for both genie-aided and CSI-based thresholds).

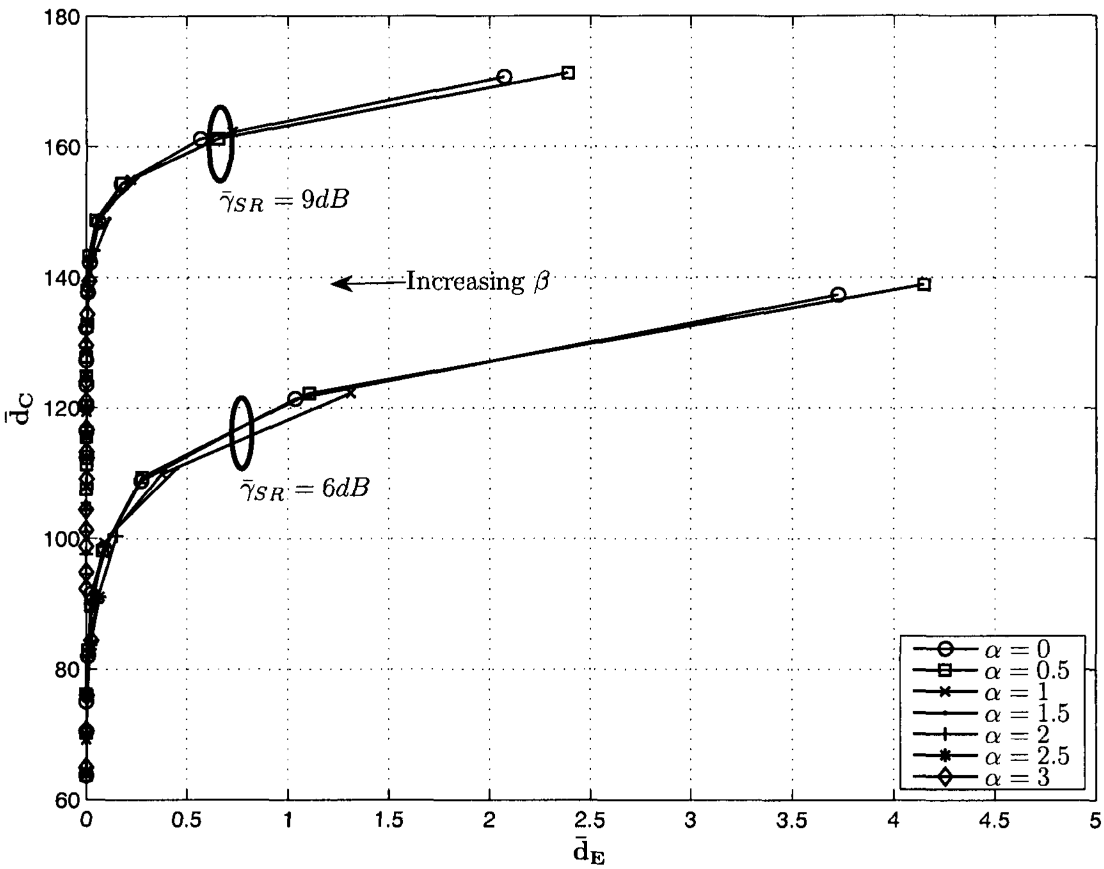

Figure 3.3: $\bar{d}_C$ vs. $\bar{d}_E$ for different threshold parameters. Each line represents a value for α while points on the lines represent variations in β.

For $\bar{\gamma}_{SR} = 6$ dB, the end-to-end bit error rate is displayed in Fig. 3.5, in addition to the upper bound derived previously for the CSI-based threshold. Compared to simple CRC, both threshold types display significant gains, with the CSI-based threshold displaying as much as 5 dB of gain (at BER $= 3 \times 10^{-3}$) over simple CRC; albeit without much diversity gain. Also notable is the error floor that is displayed when using analog-LLR forwarding and simple DF, with the latter flooring at a value

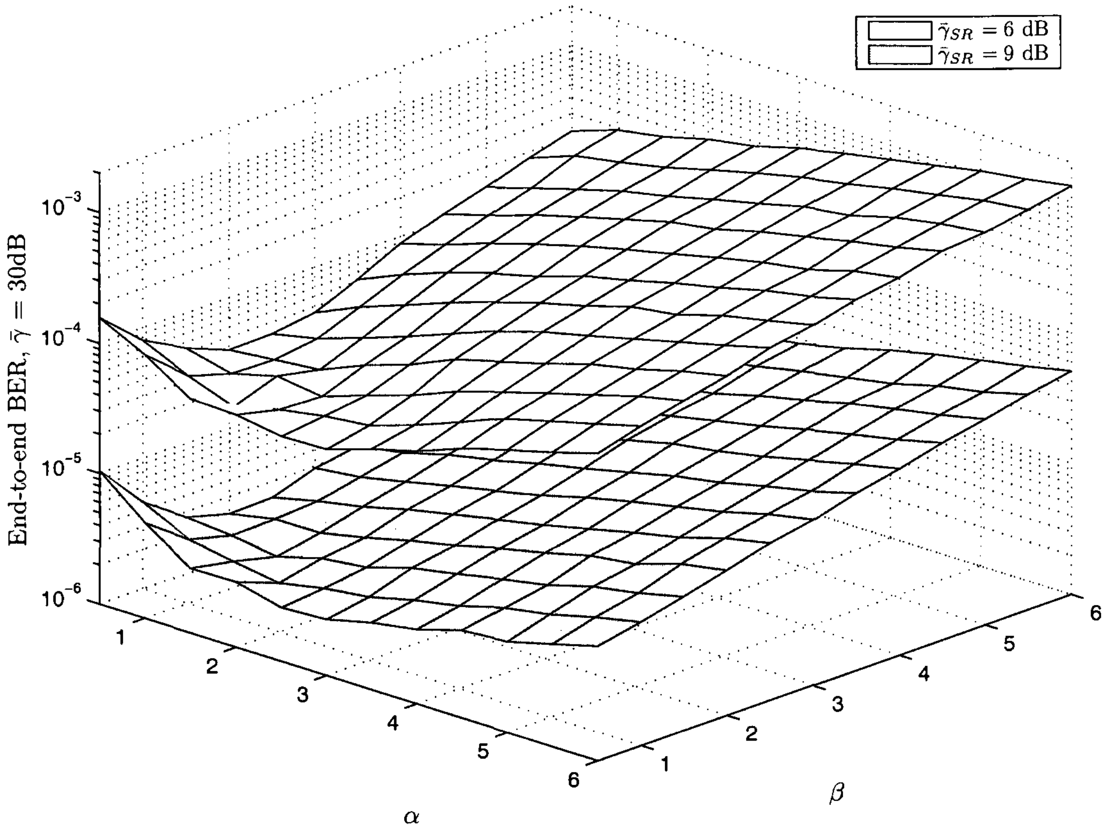

Figure 3.4: End-to-end bit error rate at $\bar{\gamma}$ = 30 dB vs. α , β. The bit error rate is found using the upper bound expression derived in (3.21) and (3.16).

an order of magnitude higher. Comparing both thresholds, we can see that the genie-aided threshold provides up to 5 dB gain (at BER $= 9 \times 10^{-4}$) over the CSI-based threshold, indicating that a more efficient threshold is possible. Finally, all techniques fall short of achieving ideal performance, owing to the low value of $\bar{\gamma}_{SR}$.

Similarly, for $\bar{\gamma}_{SR} = 9$ dB, we show simulated results in Fig. 3.6. Both threshold types display higher gains compared to simple CRC (Note that CRC does not benefit much from the increase in $\bar{\gamma}_{SR}$, since any single error in the frame triggers CRC).

The CSI-based threshold achieves both a diversity gain and a coding gain over CRC. Analog LLR relaying, however, achieves slightly better bit error rate (≈ 0.7 dB) but starts losing diversity quickly with $\bar{\gamma} > 20$ dB, after which both thresholds achieve increasing gains. Comparing both thresholds, we can see the genie-aided threshold still outperforms the proposed CSI-based threshold by a small gain until $\bar{\gamma} = 20$ dB after which the CSI-based threshold starts losing diversity. We can also note that both thresholds approach the ideal performance, with the genie-aided threshold staying within 1 dB of the ideal performance.

3.4.3 Other Relay-Destination and Source-Relay Channel Models

So far we have investigated the system in the case of quasi-static source-destination and relay-destination fading with a block-faded source-relay channel. However, we stipulate that our proposed technique still provides gains in other channel models. To illustrate the effect of different channel models on the system performance, we simulate the system in the case of *all* channels exhibiting quasi-static fading, and in the case of block-faded relay-destination and source-relay channels (both with 20 independent fades). Although the thresholds were not optimized for these cases, we nevertheless use the thresholds derived for a quasi-static relay-destination channel with the same $\bar{\gamma}_{SR}$. Obtained results are shown in Figs. 3.7 and 3.8 for all quasi-static channels with $\bar{\gamma}_{SR}$ =6 dB and 9 dB, respectively, and Figs. 3.9 and 3.10 for block faded relay-destination and source-destination channels with $\bar{\gamma}_{SR}$ =6 dB and 9

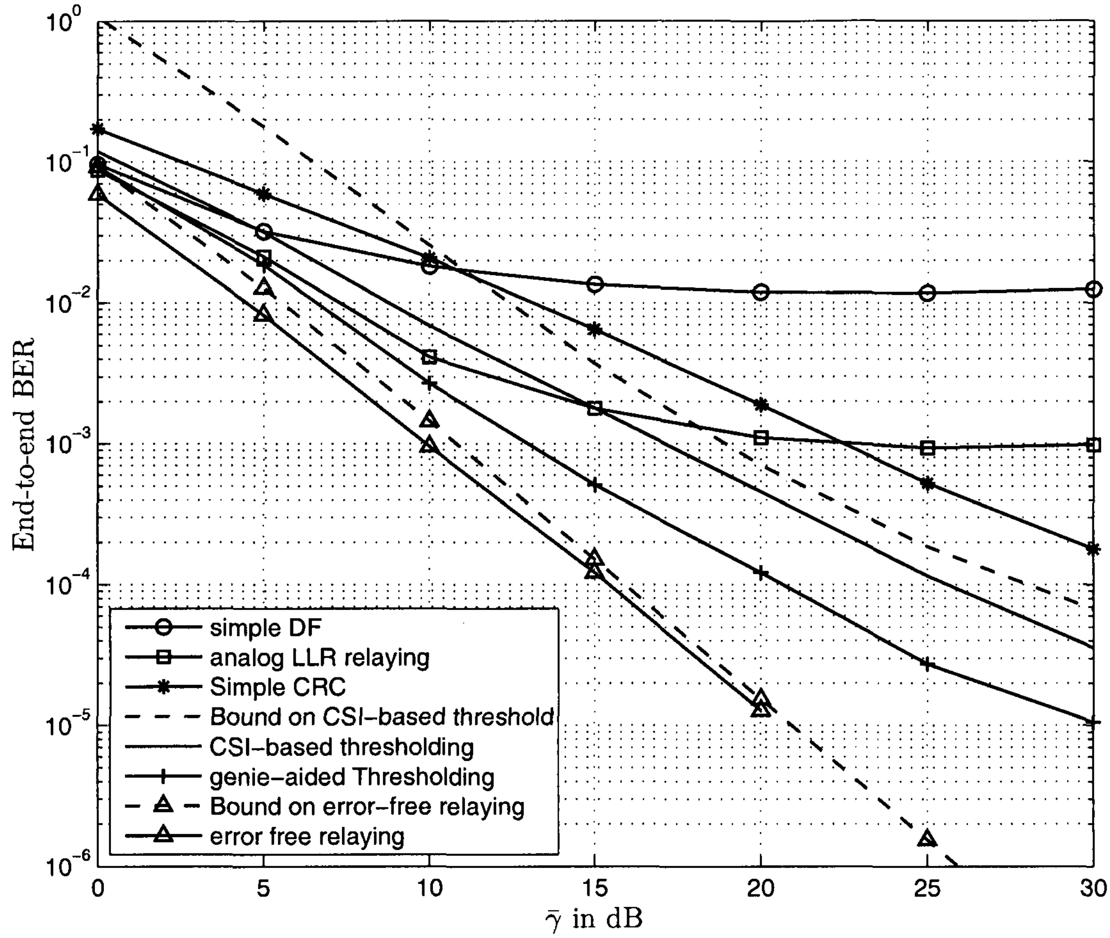

Figure 3.5: End-to-end bit error rate vs. $\bar{\gamma}$, displayed for different error propagation control techniques at the relay. $\bar{\gamma}_{SR}$ was fixed at 6 dB. Analog LLR relaying was implemented according to [1]

dB, respectively.

We can see that for the case when all channels are quasi-static, both CRC and analog LLR perform worse than the proposed thresholding. However, we see that the performance gain by thresholding reduced significantly ($\approx$ 2dB over CRC), in addition to providing no diversity gain. That is expected since if the source-channel

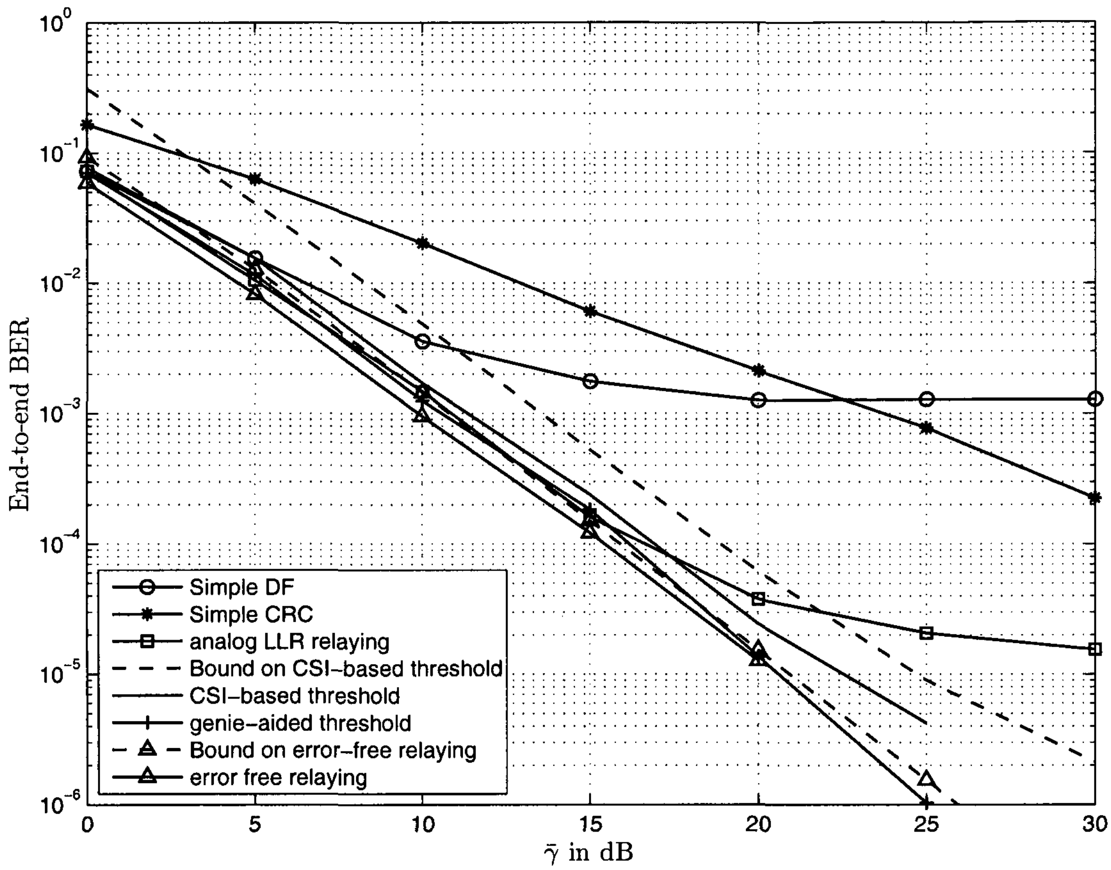

Figure 3.6: End-to-end bit error rate vs. $\bar{\gamma}$, displayed for different error propagation control techniques at the relay. $\bar{\gamma}_{SR}$ was fixed at 9 dB. Analog LLR relaying was implemented according to [1]

was bad throughout the received frame then CRC approximates the ideal decision of discarding the whole frame. Moreover, because the source-relay destination is quasi-static, we notice no significant improvement from $\bar{\gamma}_{SR}$ =6 dB to 9 dB.

When examining the case where both source-relay and relay-destination channels are block-faded, a significant performance gap is shown. Although no diversity gain is observed at $\bar{\gamma}_{SR}$ =6 dB, we still see a significant gain of 7 dB over CRC at bit

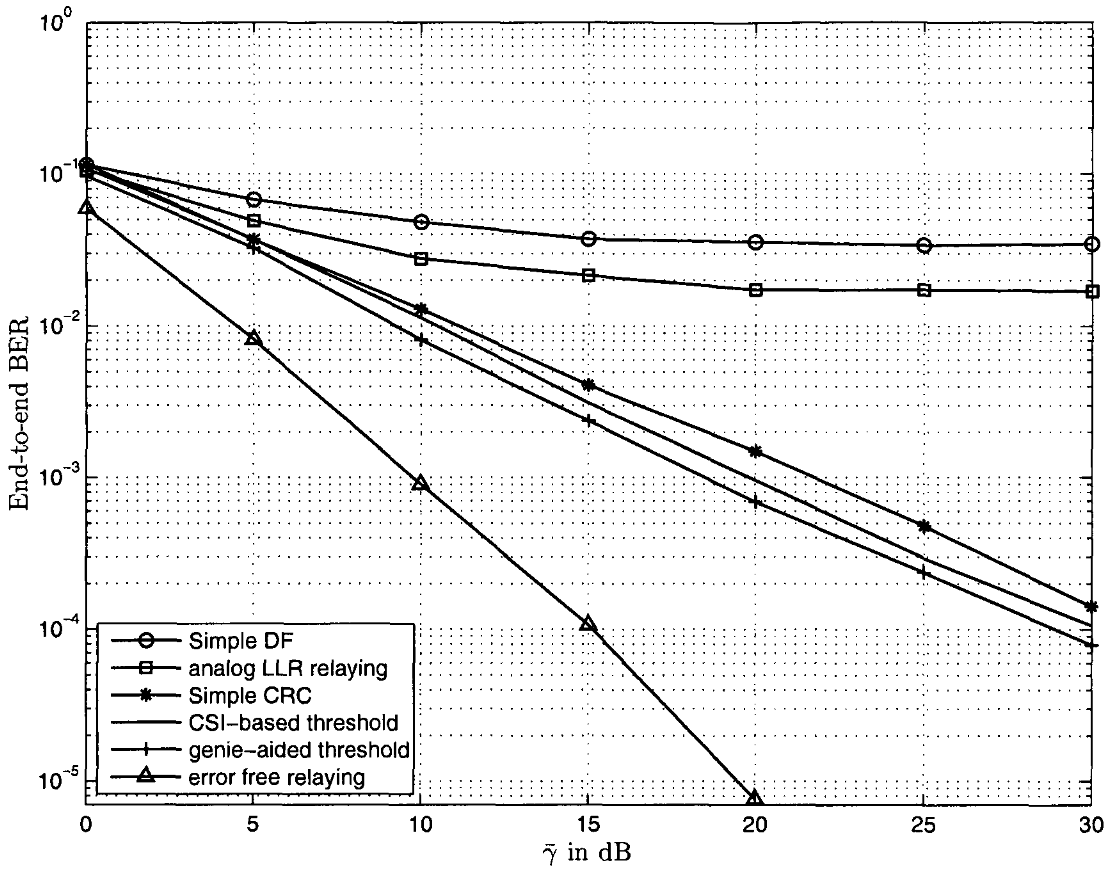

Figure 3.7: End-to-end bit error rate vs. $\bar{\gamma}$, with $\bar{\gamma}_{SR}$ fixed at 6 dB. All channels were quasi-static.

error rate of 10^{-3}, with both simple DF and analog LLR exhibiting an error floor. With increasing $\bar{\gamma}_{SR}$ to 9 dB, however, we can see both a diversity and a coding gain for thresholding over CRC and analog LLR forwarding, with analog LLR losing diversity after $\bar{\gamma}$ =10 dB, genie-aided thresholding losing diversity after $\bar{\gamma}$ =15 dB, and CSI-based thresholding losing diversity at the same point.

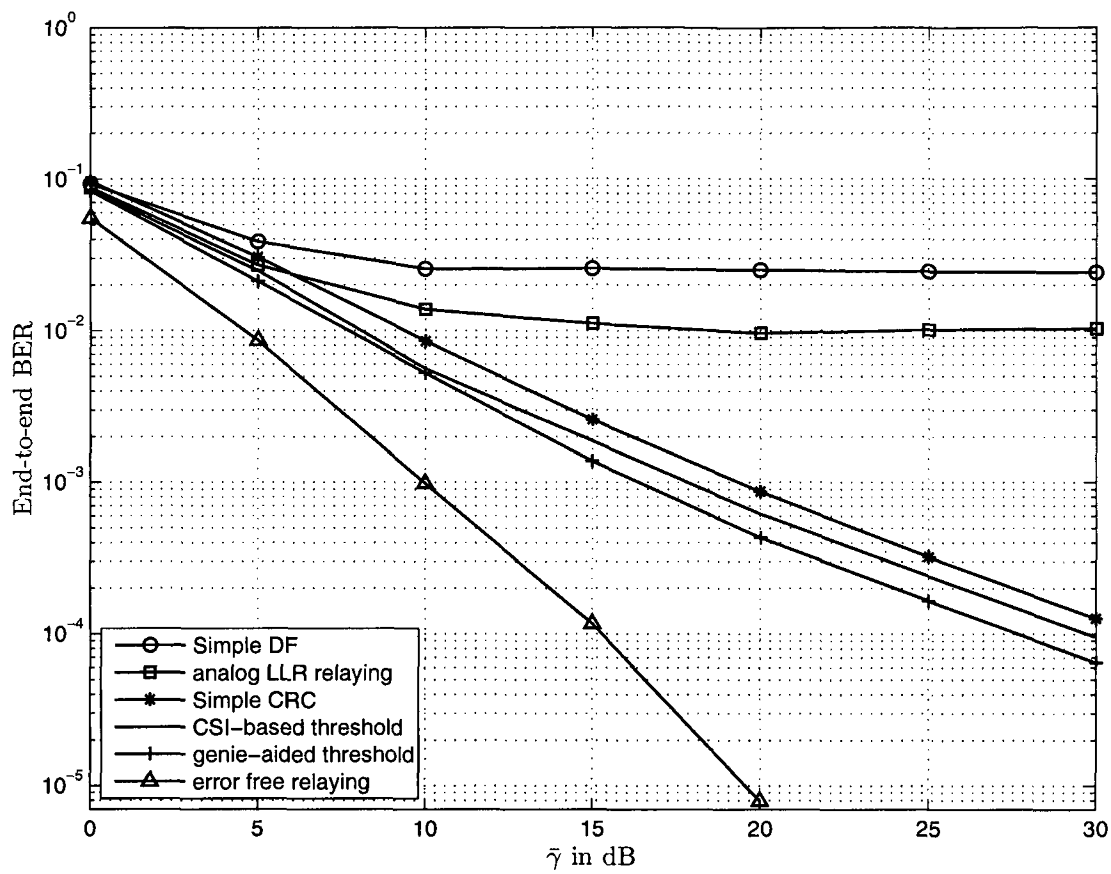

Figure 3.8: End-to-end bit error rate vs. $\bar{\gamma}$, with $\bar{\gamma}_{SR}$ fixed at 9 dB. All channels were quasi-static.

3.5 Conclusion

In this chapter, we have investigated thresholding as means to mitigate error propagation in cooperative communications. Our proposed system relied on soft estimates of bits, and used them to block unreliable bits from being forwarded to the destination. After comparing the proposed technique with just using CRC at the relay, with simple DF, and analog LLR forwarding, we can conclude that we can achieve significant improvement by using thresholding at the relay. While analog LLR forwarding and

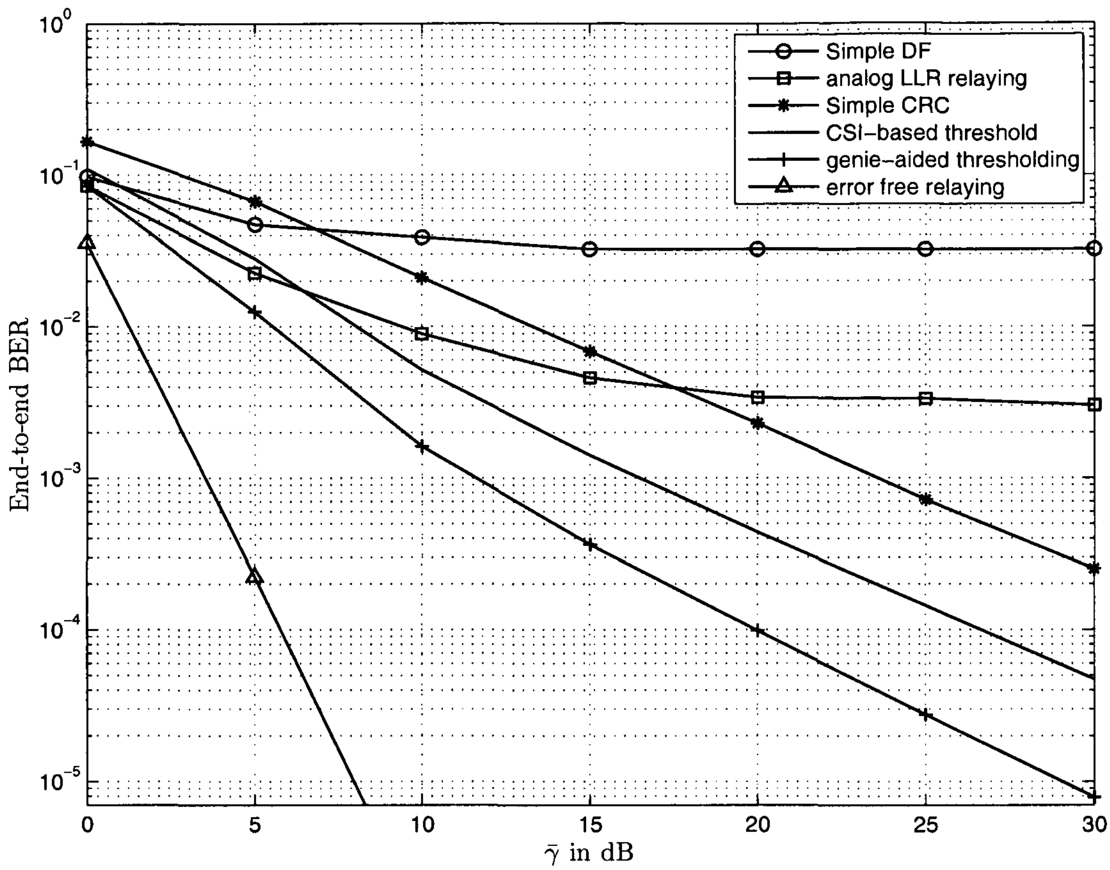

Figure 3.9: End-to-end bit error rate vs. $\bar{\gamma}$, with $\bar{\gamma}_{SR}$ fixed at 6 dB. Relay-destination channel was block-faded with 20 independent fades.

simple DF caused an error floor in the end-to-end bit error rate of the system, CRC lost too much diversity by discarding the whole frame, and our proposed technique was able to circumvent both disadvantages.

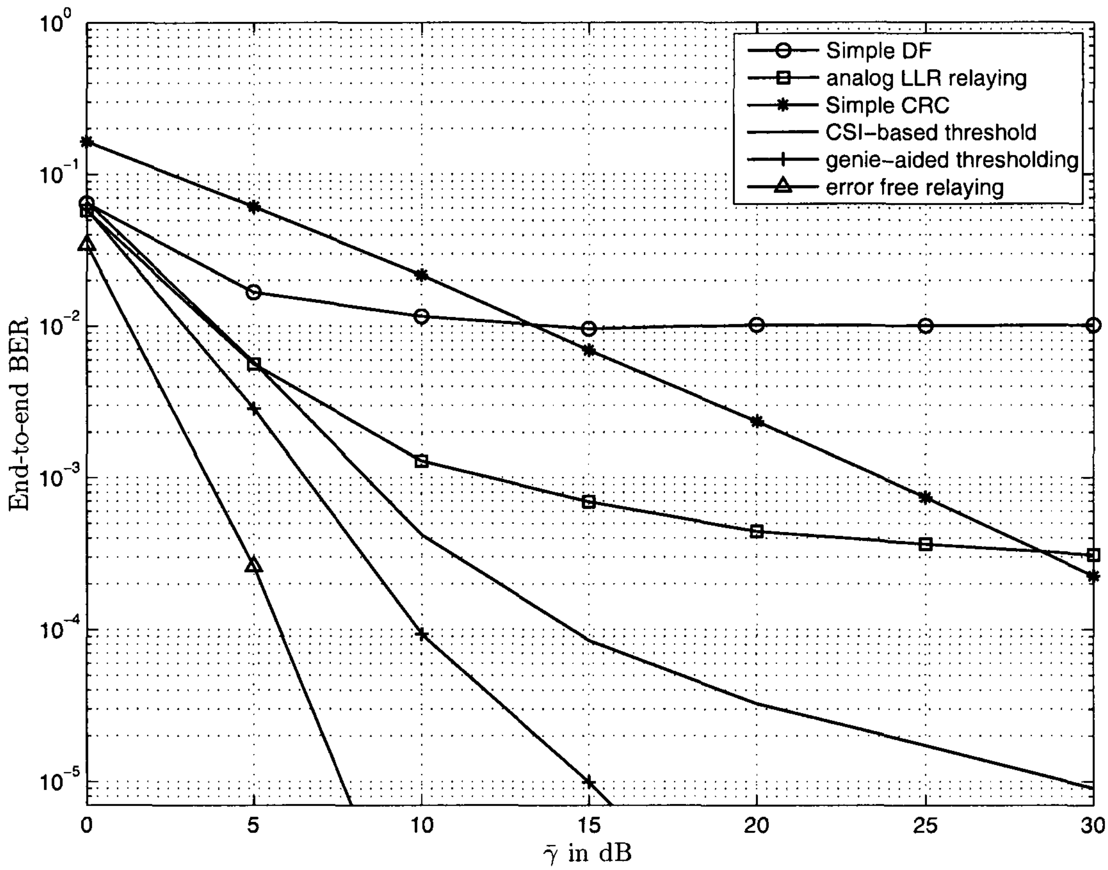

Figure 3.10: End-to-end bit error rate vs. $\bar{\gamma}$, with $\bar{\gamma}_{SR}$ fixed at 9 dB. Relay-destination channel was block-faded with 20 independent fades.

Chapter 4

Thresholding in Network-Coded Networks

In the previous chapter, we have shown the performance gain achieved by employing thresholding at the relay. We now direct our interest towards network-coded cooperative systems; in order to address the problem of limited throughput. In network-coded cooperative systems, a relay can create significant throughput by combining the destined output to two sources into one frame and broadcasting this frame to both sources simultaneously.

In this chapter, we investigate the application of the proposed thresholding technique to network-coded systems. We consider the case of a relay cooperating with two sources simultaneously using simple modulo-2 addition of the decoded bits of both sources: This is normally referred to as a two-way relay channel. Then, we investigate different scenarios of symmetric source-relay channels or asymmetric channels (whereby one source maintains a stronger channel with the relay than the other), as well as two methods of applying the LLR threshold at the relay–namely, applying the thresholds separately to the bits then combining them or applying one combined threshold over the combined bits. We analyze the performance of the system in all of these methods, which leads us to optimize the thresholds to achieve the minimum bit error rate. We show using computer simulations that applying thresholding separately yields better performance than applying one combined threshold.

Finally, we touch upon extending the application of thresholding in joint network-channel coded cooperative systems and we include simulation results that display the potential of thresholding in such scenarios.

4.1 Uncoded System Description

In this section, we assume that no channel coding is used between the terminals to simplify analysis. Later, we investigate applying the proposed technique to coded cooperative systems as displayed in [40].

For this case, we choose a system of two nodes communicating with each other through a single cooperating relay. We then apply our proposed thresholding technique at the relay to limit errors propagating to the target node.

As such, each node (also called a source) transmits one bit to the other source. We refer to the bit originating at the first source (denoted by S_1) as x_{S_1}, and to the bit originating at the first source (denoted by S_2) as x_{S_2}.For notational expedience, we assume that the bits take values $\in \{\pm 1\}$.

In addition to each source listening to the other source's bit, the relay listens to both sources' transmissions (forming $\hat{x}_{S_1}$ and $\hat{x}_{S_2}$). Then it combines both bits by adding them modulo-2. We then investigate several methods by which the relay decides whether the combined bit is reliable. If deemed reliable, the relay broadcasts the combined bit to both sources, otherwise it stays silent.

Thus, S_1 obtains two instances of x_{S_2}–one from listening to the transmission of S_2 and one from decoding the output of the relay by adding it modulo-2 to x_{S_1}, and vice versa for S_2. Each source then combines both copies using MRC to obtain the final estimate of the other sources' bit. See Fig.4.1 for a block diagram of the system under study.

We divide the entire transmission period into two stages–the broadcast stage followed by the cooperation stage.

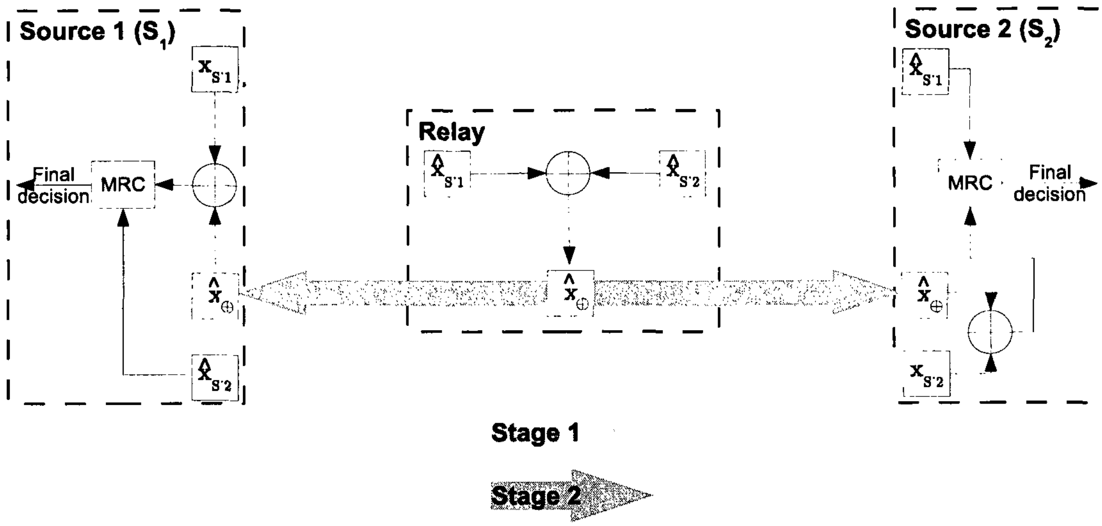

Figure 4.1: System block diagram for the case of non-channel-coded network-coded cooperation

4.1.1 The Broadcast Stage

In this stage, each source broadcasts its respective bit (through orthogonal channels). We express the received bits at both sources and at the relay as

$$r_{S_1R} = \sqrt{E_b}h_{S_1R}x_{S_1} + n_{S_1R}, \tag{4.1}$$

$$r_{S_2R} = \sqrt{E_b}h_{S_2R}x_{S_2} + n_{S_2R}, \tag{4.2}$$

$$r_{S_1S_2} = \sqrt{E_b}h_{S_1S_2}x_{S_1} + n_{S_1S_2}, \tag{4.3}$$

$$r_{S_2S_1} = \sqrt{E_b}h_{S_2S_1}x_{S_1} + n_{S_2S_1}, \tag{4.4}$$

where r_{S_1R} and r_{S_2R} are the received bits at the relay from S_1 and S_2, respectively, $r_{S_1S_2}$ and $r_{S_2S_1}$ are the bits received at S_2 from S_1 and vice versa, respectively. E_b

denotes the transmitted energy per bit. h indicates the associated fading, with subscripts indicating the specific channel. x_{S_1} and x_{S_2} denote the bits transmitted by S_1 and S_2, respectively. Finally, n_{S_1R}, n_{S_2R}, $n_{S_1S_2}$ and $n_{S_2S_1}$ are complex AWGN samples with per-dimension variance of $N_0/2$. For the rest of the thesis, we assume BPSK modulation throughout, thus $x_{S_1}, x_{S_2} \in \{\pm 1\}$.

4.1.2 The Cooperation Stage

In this stage, the relay assists the individual sources by re-transmitting their respective bits to the opposite sources. We explain next two possible scenarios–one where the relay cooperates individually with each source, and the other where the relay cooperates with both sources simultaneously using network coding.

Individual Cooperation

If the relay is to cooperate with S_1 and S_2 individually (thus needing two orthogonal channels) the relay would then be transmitting the bit of S_2 to S_1 over one channel, and vice versa over the other channel. The detected bits at the relay are found by maximum likelihood (ML) detection, namely,

$$\begin{aligned} \hat{x}_{S_1} &= sign\left(\Re\left\{r_{S_1R}h^*_{S_1R}\right\}\right), \\ \hat{x}_{S_2} &= sign\left(\Re\left\{r_{S_2R}h^*_{S_2R}\right\}\right), \end{aligned}$$

for the detected bit of x_{S_1}, x_{S_2}, respectively, where r_{S_1R} and r_{S_1R} are expressed in (4.1) and (4.2), respectively, $(\cdot)^*$ indicates complex conjugation, and $\Re\{\cdot\}$ indicates taking the real part. Hence, the received bits at both sources can be expressed as

$$
\begin{aligned}
r_{RS_1} &= \sqrt{E_b} h_{RS_1} \hat{x}_{S_2} + n_{RS_1}, & (4.5)\\
r_{RS_2} &= \sqrt{E_b} h_{RS_2} \hat{x}_{S_1} + n_{RS_2}, & (4.6)
\end{aligned}
$$

with variable definitions similar to that of (4.1)-(4.4). Finally, each source combines the two received copies of the other source's bit using maximum ratio combining (MRC). Consecutively, the final decided bit at each source is expressed as

$$
\begin{aligned}
y_1 &= sign\left(\Re\left\{r_{S_1S_2} h^*_{S_1S_2} + r_{RS_2} h^*_{RS_2}\right\}\right),\\
y_2 &= sign\left(\Re\left\{r_{S_2S_1} h^*_{S_2S_1} + r_{RS_1} h^*_{RS_1}\right\}\right).
\end{aligned}
$$

where y_1 and y_2 are the final detected bits of S_1 and S_2, respectively (detected at S_2 and S_1, respectively).

Using Network Coding

If the relay is to cooperate with S_1 and S_2 simultaneously (using network coding) the relay would then be transmitting the exclusive-or (XOR) of S_2 and S_1 over one channel; thus saving one channel utilization. That is,

$$\hat{x}_\oplus = \hat{x}_{S_1} \oplus \hat{x}_{S_2} = -\left(\hat{x}_{S_1}\hat{x}_{S_2}\right),$$

where the second equality follows from $\hat{x}_{S_1}, \hat{x}_{S_2} \in \{\pm 1\}$. It follows directly that the received bits at both sources are thus

$$r_{RS_1} = \sqrt{E_b} h_{RS_1} \hat{x}_{\oplus} + n_{RS_1}, \tag{4.7}$$

$$r_{RS_2} = \sqrt{E_b} h_{RS_2} \hat{x}_{\oplus} + n_{RS_2}. \tag{4.8}$$

Then, each source combines the received network-coded bit by modulo-2 adding it with its own bit, followed by MRC with the bit from the broadcast stage. Consequently, the final decided bit at each source is expressed as

$$\begin{aligned} \hat{x}_1 &= sign\left(\Re\left\{r_{S_1S_2} h^*_{S_1S_2} - x_{S_2} r_{RS_2} h^*_{RS_2}\right\}\right), \\ \hat{x}_2 &= sign\left(\Re\left\{r_{S_2S_1} h^*_{S_2S_1} - x_{S_1} r_{RS_1} h^*_{RS_1}\right\}\right), \end{aligned}$$

where $\hat{x}_1$ and $\hat{x}_2$ are the final detected bits of S_1 and S_2, respectively (detected at S_2 and S_1, respectively).

4.2 Thresholding Protocol

In the previous section, we detailed the uncoded two-way cooperative network under study. To combat the effect of error propagation, the authors in [20] proposed to use a reliability threshold at the relay before transmitting to the sources. In the event that the reliability of the bit is below the set threshold, the relay stays silent and transmits nothing, otherwise, the hard-coded bit is sent. We summarize the protocol for the non-network-coded in the following section.

4.2.1 Individual Cooperation

The authors in [20] proposed to find the reliability of the received bit at the relay, expressed in terms of the LLR of the bit, which was formally defined as.

$$\begin{aligned}
\Lambda_{\hat{x}_{S_1}} &= \log \frac{Pr\left[x_{S_1}=1\right]}{Pr\left[x_{S_1}=-1\right]} = 4\sqrt{E_b}\left(\Re\left\{r_{S_1R}h^*_{S_1R}\right\}\right), \\
\Lambda_{\hat{x}_{S_2}} &= \log \frac{Pr\left[x_{S_2}=1\right]}{Pr\left[x_{S_2}=-1\right]} = 4\sqrt{E_b}\left(\Re\left\{r_{S_2R}h^*_{S_2R}\right\}\right),
\end{aligned}$$

for the LLR of the bits received from S_1, S_2, respectively, where $Pr[\cdot]$ indicates the probability of the enclosed event. For the rest of the thesis, all logarithms are taken to the natural base. Then, if the LLR exceeds in magnitude a preset threshold, then the bit is transmitted. Otherwise, the bit is nulled and not forwarded to the destination. Namely,

$$\hat{x}_{S_1} = \begin{cases} sign\left(\Re\left\{r_{S_1R}h^*_{S_1R}\right\}\right), & \left|\Lambda_{\hat{x}_{S_1}}\right| > T_{S_1} \\ 0, & \left|\Lambda_{\hat{x}_{S_1}}\right| \leq T_{S_1} \end{cases},$$

where T_{S_1} is the threshold set for forwarding bits of S_1, and similarly for $\hat{x}_{S_2}$. It was also shown in [20] that the optimal thresholds T_{S_1} and T_{S_2} in the case of individual cooperation can be expressed as

$$
\begin{aligned}
T_{S_1}^{opt} &= \log\left(\frac{P_{S_2}^{(X)} - P_{S_2}^{(MRC)}}{P_{S_2}^{(SD)}} - 1\right), \\
T_{S_2}^{opt} &= \log\left(\frac{P_{S_1}^{(X)} - P_{S_1}^{(MRC)}}{P_{S_1}^{(SD)}} - 1\right),
\end{aligned}
$$

respectively, where $P_{S_1}^{(X)}$ indicates the bit error rate at S_1 given that the relay forwards an incorrect bit to S_1, $P_{S_1}^{(MRC)}$ indicates the bit error rate at S_1 given that the relay forwards a correct bit to S_1, and $P_{S_1}^{(SD)}$ indicates the bit error rate at S_1 given that the relay stays silent. The definitions of $P_{S_2}^{(X)}$, $P_{S_2}^{(MRC)}$, and $P_{S_2}^{(SD)}$ are similarly defined. These thresholds simultaneously achieve minimum bit error rates at S_1, S_2.

4.2.2 Using Network Coding

The challenge in thresholding when using network coding is that thresholding can be implemented at the individual-bit level or at the network-coded-bit level. We elaborate on this next.

Individual-bit Thresholding

Using individual-bit thresholding is similar to thresholding in the individual cooperation case. When finding $\hat{x}_{\oplus}$, however, the output is nulled when any of the two bits are nulled. Namely,

$$\hat{x}_{\oplus} = \begin{cases} -\left(\hat{x}_{S_1}\hat{x}_{S_2}\right), & \left|\Lambda_{\hat{x}_{S_1}}\right| > T_{S_1} \text{ and } \left|\Lambda_{\hat{x}_{S_2}}\right| > T_{S_2} \\ 0, & \text{otherwise} \end{cases}.$$

This thresholding scheme requires setting two thresholds T_{S_1}, T_{S_2} at the relay. We discuss the optimal thresholds for this case later in Section 4.3.

Network-coded-bit Thresholding

From $\Lambda_{\hat{x}_{S_1}}, \Lambda_{\hat{x}_{S_2}}$ we can find the LLR of the combined bit (denoted by $\Lambda_{\hat{x}_{\oplus}}$) as follows

$$\begin{aligned} \Lambda_{\hat{x}_{\oplus}} &= \log \frac{Pr\left[x_{\oplus} = 1\right]}{Pr\left[x_{\oplus} = -1\right]} \\ &= \log \frac{Pr\left[x_{S_1} = 1\right] Pr\left[x_{S_2} = -1\right] + Pr\left[x_{S_1} = -1\right] Pr\left[x_{S_2} = 1\right]}{Pr\left[x_{S_1} = 1\right] Pr\left[x_{S_2} = 1\right] + Pr\left[x_{S_1} = -1\right] Pr\left[x_{S_2} = -1\right]} \\ &= \log \frac{\frac{Pr\left[x_{S_1}=1\right]}{Pr\left[x_{S_1}=-1\right]} + \frac{Pr\left[x_{S_2}=1\right]}{Pr\left[x_{S_2}=-1\right]}}{\frac{Pr\left[x_{S_1}=1\right]}{Pr\left[x_{S_1}=-1\right]} \frac{Pr\left[x_{S_2}=1\right]}{Pr\left[x_{S_2}=-1\right]} + 1} \\ &= \log \frac{e^{\Lambda_{\hat{x}S_1}} + e^{\Lambda_{\hat{x}S_2}}}{e^{\Lambda_{\hat{x}S_1}} e^{\Lambda_{\hat{x}S_2}} + 1} \\ \Lambda_{\hat{x}_{\oplus}} &= \log\left(e^{\Lambda_{\hat{x}S_1}} + e^{\Lambda_{\hat{x}S_2}}\right) - \log\left(e^{\Lambda_{\hat{x}S_1} + \Lambda_{\hat{x}S_2}} + 1\right). \end{aligned}$$

Hence, we can set a single threshold (denoted by $T_{\oplus}$) and apply it to the combined bits (we derive the optimal $T_{\oplus}$ for this case in Section 4.3.) Formally, such a rule is expressed as

$$\hat{x}_{\oplus} = \begin{cases} -\left(\hat{x}_{S_1}\hat{x}_{S_2}\right), & \left|\Lambda_{\hat{x}_{\oplus}}\right| > T_{\oplus} \\ 0, & \text{otherwise} \end{cases}.$$

4.3 Performance Analysis

In this section, we analyze the performance of our proposed thresholding scheme in terms of BER. We first briefly discuss the analysis in [20] covering the case of individual-bit thresholding. Then we apply the analysis for the case of network-coded-bit thresholding. For both cases, we distinguish six events at the relay with regards to the forwarded bits–$\mathcal{E}_{eS_1}$ indicating an error in decoding the bit for S_1 at the relay, $\mathcal{E}_{xS_1}$ indicating a nulled bit for S_1, and $\mathcal{E}_{cS_1}$ indicating a correctly-decoded bit for S_1 (with their counterparts for S_2).

4.3.1 Individual Cooperation

Although not part of the described If the relay is forwarding bits to S_1, S_2 separately, we can formally define $\mathcal{E}_{eS_1}$, $\mathcal{E}_{xS_1}$, $\mathcal{E}_{cS_1}$, $\mathcal{E}_{eS_2}$, $\mathcal{E}_{xS_2}$ and $\mathcal{E}_{cS_2}$ as

$$\begin{aligned}
\mathcal{E}_{eS_1} &: \left|\Lambda_{\hat{x}_{S_1}}\right| > T_{S_1}, sign\left(\Lambda_{\hat{x}_{S_1}}\right) \neq x_{S_1}, \\
\mathcal{E}_{cS_1} &: \left|\Lambda_{\hat{x}_{S_1}}\right| > T_{S_1}, sign\left(\Lambda_{\hat{x}_{S_1}}\right) = x_{S_1}, \\
\mathcal{E}_{xS_1} &: \left|\Lambda_{\hat{x}_{S_1}}\right| \leq T_{S_1}, \\
\mathcal{E}_{eS_2} &: \left|\Lambda_{\hat{x}_{S_2}}\right| > T_{S_2}, sign\left(\Lambda_{\hat{x}_{S_2}}\right) \neq x_{S_2}, \\
\mathcal{E}_{cS_2} &: \left|\Lambda_{\hat{x}_{S_2}}\right| > T_{S_2}, sign\left(\Lambda_{\hat{x}_{S_2}}\right) = x_{S_2}, \\
\text{and } \mathcal{E}_{xS_2} &: \left|\Lambda_{\hat{x}_{S_2}}\right| \leq T_{S_2}, \qquad (4.9)
\end{aligned}$$

respectively. Consequently, the bit error rate at S_1 and S_2 is expressed as

$$\begin{aligned}
P_{S_1}^{(e)} &= P_{S_1}^{(SD)} Pr\left[\mathcal{E}_{xS_2}\right] + P_{S_1}^{(MRC)} Pr\left[\mathcal{E}_{cS_2}\right] + P_{S_1}^{(X)} Pr\left[\mathcal{E}_{eS_2}\right], \\
&= Pr\left[y_2 \neq x_2\right] \qquad (4.10) \\
P_{S_2}^{(e)} &= P_{S_2}^{(SD)} Pr\left[\mathcal{E}_{xS_1}\right] + P_{S_2}^{(MRC)} Pr\left[\mathcal{E}_{cS_1}\right] + P_{S_2}^{(X)} Pr\left[\mathcal{E}_{eS_1}\right], \\
&= Pr\left[y_1 \neq x_1\right] \qquad (4.11)
\end{aligned}$$

respectively, where $P_{S_1}^{(X)}$, $P_{S_1}^{(MRC)}$, $P_{S_1}^{(SD)}$, $P_{S_2}^{(X)}$, $P_{S_2}^{(MRC)}$, and $P_{S_2}^{(SD)}$ were defined earlier.

4.3.2 Network-coded Cooperation

For this type of cooperation, it follows that a nulled bit from the relay is equivalent to nulled bits to both sources in the individual cooperation case. Furthermore, an incorrect bit is equivalent to forwarding incorrect bits to both sources in the individual cases, as is the case for a correct bit. Hence, the components of each pair of $(\mathcal{E}_{eS_1}, \mathcal{E}_{eS_2})$, $(\mathcal{E}_{xS_1}, \mathcal{E}_{xS_2})$, and $(\mathcal{E}_{cS_1}, \mathcal{E}_{cS_2})$ are equivalent events.

We have previously distinguished two cases of thresholding for the case of network-coded cooperation. Next, we go into the performance analysis for both cases.

Individual-bit Thresholding

In this case of thresholding, the definitions for $\mathcal{E}_{eS_{1,2}}$, $\mathcal{E}_{xS_{1,2}}$ and $\mathcal{E}_{cS_{1,2}}$ become

$$\begin{aligned}
\mathcal{E}_{eS_{1,2}} \quad &: \quad \left|\Lambda_{\hat{x}_{S_1}}\right| > T_{S_1}, \left|\Lambda_{\hat{x}_{S_2}}\right| > T_{S_2}, \\
&\quad \left(sgn\left(\Lambda_{\hat{x}_{S_1}}\right) sgn\left(\Lambda_{\hat{x}_{S_2}}\right)\right) \neq \left(x_{S_1} x_{S_2}\right), \\
\mathcal{E}_{cS_{1,2}} \quad &: \quad \left|\Lambda_{\hat{x}_{S_1}}\right| > T_{S_1}, \left|\Lambda_{\hat{x}_{S_2}}\right| > T_{S_2}, \\
&\quad \left(sgn\left(\Lambda_{\hat{x}_{S_1}}\right) sgn\left(\Lambda_{\hat{x}_{S_2}}\right)\right) = \left(x_{S_1} x_{S_2}\right), \\
\text{and } \mathcal{E}_{xS_{1,2}} \quad &: \quad \left|\Lambda_{\hat{x}_{S_1}}\right| \leq T_{S_1} \text{ OR } \left|\Lambda_{\hat{x}_{S_2}}\right| \leq T_{S_2},
\end{aligned} \tag{4.12}$$

respectively. We use the following probability distributions, derived in [20] to help us in finding the optimum T_{S_1}, T_{S_2},

$$
\begin{aligned}
f_{z_1}(z) &= \frac{1+e^{4z}}{\sqrt{\beta_1^2+\beta_1}} e^{-2\left(\sqrt{1+\beta_1^{-1}}+1\right)z}, \\
f_{z_2}(z) &= \frac{1+e^{4z}}{\sqrt{\beta_2^2+\beta_2}} e^{-2\left(\sqrt{1+\beta_2^{-1}}+1\right)z},
\end{aligned}
$$

where $z_1 \triangleq \frac{\left|\Lambda_{\hat{x}_{S_1}}\right|}{4}$, $z_2 \triangleq \frac{\left|\Lambda_{\hat{x}_{S_2}}\right|}{4}$, and $\beta_1 \triangleq E\left[|h_{S_1R}|^2\right] E_b, \beta_2 \triangleq E\left[|h_{S_2R}|^2\right] E_b$.

It follows then that the probabilities of $\mathcal{E}_{xS_{1,2}}$, $\mathcal{E}_{cS_{1,2}}$, and $\mathcal{E}_{eS_{1,2}}$ evaluate to, based on the definitions in (4.12),

$$
\begin{aligned}
Pr\left[\mathcal{E}_{xS_{1,2}}\right] &= Pr\left[\left|\Lambda_{\hat{x}_{S_1}}\right| \leq T_{S_1} \cup \left|\Lambda_{\hat{x}_{S_2}}\right| \leq T_{S_2}\right] \\
&= Pr\left[\left|\Lambda_{\hat{x}_{S_1}}\right| \leq T_{S_1}\right] + Pr\left[\left|\Lambda_{\hat{x}_{S_2}}\right| \leq T_{S_2}\right] \\
&\quad - \left(Pr\left[\left|\Lambda_{\hat{x}_{S_1}}\right| \leq T_{S_1}\right] Pr\left[\left|\Lambda_{\hat{x}_{S_2}}\right| \leq T_{S_2}\right]\right) \\
&= \int_0^{T_{S_1}/4} f_{z_1}(z)dz + \int_0^{T_{S_2}/4} f_{z_2}(z)dz \\
&\quad - \left(\int_0^{T_{S_1}/4} f_{z_1}(z)dz\right)\left(\int_0^{T_{S_2}/4} f_{z_2}(z)dz\right), \qquad (4.13) \\
Pr\left[\mathcal{E}_{cS_{1,2}}\right] &= 1 - Pr\left[\mathcal{E}_{eS_{1,2}}\right], \qquad (4.14)
\end{aligned}
$$

and

$$\begin{aligned}
Pr\left[\mathcal{E}_{eS_{1,2}}\right] &= Pr\left[\left(sgn\left(\Lambda_{\hat{x}_{S_1}}\right) sgn\left(\Lambda_{\hat{x}_{S_2}}\right)\right) \neq \left(x_{S_1} x_{S_2}\right)\right. \\
&\quad \left. \mid \left|\Lambda_{\hat{x}_{S_1}}\right| > T_{S_1}, \left|\Lambda_{\hat{x}_{S_2}}\right| > T_{S_2}\right] \\
&= Pr\left[sgn\left(\Lambda_{\hat{x}_{S_1}}\right) \neq x_{S_1} \mid \left|\Lambda_{\hat{x}_{S_1}}\right| > T_{S_1}\right] \\
&\quad \cdot Pr\left[sgn\left(\Lambda_{\hat{x}_{S_2}}\right) = x_{S_2} \mid \left|\Lambda_{\hat{x}_{S_2}}\right| > T_{S_2}\right] \\
&\quad + Pr\left[sgn\left(\Lambda_{\hat{x}_{S_1}}\right) = x_{S_1} \mid \left|\Lambda_{\hat{x}_{S_1}}\right| > T_{S_1}\right] \\
&\quad \cdot Pr\left[sgn\left(\Lambda_{\hat{x}_{S_2}}\right) \neq x_{S_2} \mid \left|\Lambda_{\hat{x}_{S_2}}\right| > T_{S_2}\right] \\
&= \left(\int\limits_{T_{S_1}/4}^{\infty} \frac{f_{z_1}(z)}{1+e^{4z}} dz\right)\left(1 - \int\limits_{T_{S_2}/4}^{\infty} \frac{f_{z_2}(z)}{1+e^{4z}} dz\right) \\
&\quad + \left(1 - \int\limits_{T_{S_1}/4}^{\infty} \frac{f_{z_1}(z)}{1+e^{4z}} dz\right)\left(\int\limits_{T_{S_2}/4}^{\infty} \frac{f_{z_2}(z)}{1+e^{4z}} dz\right),
\end{aligned} \tag{4.15}$$

respectively, where the last equality follows from the following equality

$$Pr\left[sgn\left(\Lambda_{\hat{x}_{S_1}}\right) \neq x_{S_1} \mid \Lambda_{\hat{x}_{S_1}}\right] = \frac{1}{1+e^{\left|\Lambda_{\hat{x}_{S_1}}\right|}}$$

which was proven in [41, (11)].

Network-coded-bit Thresholding

In this case of thresholding, the definitions for $\mathcal{E}_{eS_{1,2}}$, $\mathcal{E}_{xS_{1,2}}$ and $\mathcal{E}_{cS_{1,2}}$ become

$$\begin{aligned}
\mathcal{E}_{eS_{1,2}} \quad &: \quad \left|\Lambda_{\hat{x}_{\oplus}}\right| > T_{\oplus}, \\
& \quad \left(sgn\left(\Lambda_{\hat{x}_{S_1}}\right) sgn\left(\Lambda_{\hat{x}_{S_2}}\right)\right) \neq \left(x_{S_1} x_{S_2}\right), \\
\mathcal{E}_{cS_{1,2}} \quad &: \quad \left|\Lambda_{\hat{x}_{\oplus}}\right| > T_{\oplus}, \\
& \quad \left(sgn\left(\Lambda_{\hat{x}_{S_1}}\right) sgn\left(\Lambda_{\hat{x}_{S_2}}\right)\right) = \left(x_{S_1} x_{S_2}\right), \\
\text{and } \mathcal{E}_{xS_{1,2}} \quad &: \quad \left|\Lambda_{\hat{x}_{\oplus}}\right| \leq T_{\oplus},
\end{aligned} \tag{4.16}$$

respectively. By denoting the PDF of the combined LLR as $f_{z_{\oplus}}(z)$, we can express the probabilities of $\mathcal{E}_{eS_{1,2}}$, $\mathcal{E}_{xS_{1,2}}$ and $\mathcal{E}_{cS_{1,2}}$ as

$$\begin{aligned}
Pr\left[\mathcal{E}_{xS_{1,2}}\right] &= \int_{0}^{T_{\oplus}/4} f_{z_{\oplus}}(z) dz, \\
Pr\left[\mathcal{E}_{eS_{1,2}}\right] &= \int_{T_{\oplus}/4}^{\infty} \frac{f_{z_{\oplus}}(z)}{1+e^{4z}} dz, \\
\text{and } Pr\left[\mathcal{E}_{cS_{1,2}}\right] &= 1 - Pr\left[\mathcal{E}_{eS_{1,2}}\right],
\end{aligned} \tag{4.17}$$

respectively. We note here that we did not obtain a closed-form expression for $f_{z_{\oplus}}(z)$, which is not needed to obtain the optimum $T_{\oplus}$.

4.3.3 Optimal Thresholds

In this section, we obtain the optimal thresholds at the relay for both cases of network-coded cooperation. Namely, with individual bit thresholding, and combined-bit thresholding.

Individual-bit thresholding

We can find the optimal thresholds (optimized for minimum $P_{S_1}^{(e)}$) by solving the set of equations for T_{S_1}, T_{S_2}

$$\frac{\partial P_{S_1}^{(e)}}{\partial T_{S_1}} = 0, \frac{\partial P_{S_1}^{(e)}}{\partial T_{S_2}} = 0,$$

where $P_{S_1}^{(e)}$ is expressed in (4.10), and using event probabilities shown in (4.15). Finally, expressions for $P^{(MRC)}$, $P^{(X)}$ and $P^{(SD)}$ can be found in [20]: $(A \cdot 10), (A \cdot 14)$ and $(A \cdot 19)$, respectively. By using numerical integration to evaluate the expressions in (4.15), we obtain all elements of $P_{S_1}^{(e)}$ and $P_{S_2}^{(e)}$; allowing us to obtain their numerical values for a specific (T_{S_1}, T_{S_2}) pair. Finally, by using a numerical optimization algorithm (such as gradient descent), we obtain the optimal pair of (T_{S_1}, T_{S_2}) (denoted as $(T_{S_1}^{opt}, T_{S_2}^{opt})$, respectively) optimized for either minimum $P_{S_1}^{(e)}$ *or* $P_{S_2}^{(e)}$.

Combined-bit thresholding

To find the optimal threshold in this case, we need to differentiate (4.10) *or* (4.11) with respect to $T_{\oplus}$ and equate the resultant to zero, to obtain the optimal threshold for minimum $P_{S_1}^{(e)}$ *or* $P_{S_2}^{(e)}$, respectively, which is expressed as

$$\begin{aligned}&\frac{\partial P_{S_1}^{(e)}}{\partial T_\oplus} = 0 \Rightarrow \\ &\quad P_{S_1}^{(SD)} \frac{\partial}{\partial T_\oplus} \left(Pr \left[\mathcal{E}_{xS_{1,2}} \right] \right) + P_{S_1}^{(MRC)} \frac{\partial}{\partial T_\oplus} \left(Pr \left[\mathcal{E}_{cS_{1,2}} \right] \right) \\ &\quad + P_{S_1}^{(X)} \frac{\partial}{\partial T_\oplus} \left(Pr \left[\mathcal{E}_{eS_{1,2}} \right] \right) = 0,\end{aligned}$$

for the case of optimizing the threshold for minimum $P_{S_1}^{(e)}$, where event probabilities used are shown in (4.17). This expression, after some algebraic manipulation, simplifies to

$$\left(P_{S_1}^{(SD)} + \frac{P_{S_1}^{(MRC)} - P_{S_1}^{(X)}}{1 + e^{T_\oplus}} \right) \frac{f_{z_\oplus}\left(\frac{T_\oplus}{4}\right)}{4} = 0.$$

This yields the following solution to the optimal threshold (to achieve minimum $P_{S_1}^{(e)}$

$$T_\oplus^{opt} = \log \left(\frac{P_{S_1}^{(X)} - P_{S_1}^{(MRC)}}{P_{S_1}^{(SD)}} - 1 \right). \tag{4.18}$$

We can follow the same procedure to set $T_\oplus$ to achieve minimum $P_{S_2}^{(e)}$, which can evaluate to a different value.

4.4 Simulation Results

The system was simulated as a relay cooperating with two sources using network-coded bits. We simulated both thresholding types in addition to the cases of no cooperation from relay, perfect cooperation from relay (assuming all relayed bits are correct), and without any thresholding at the relay. Throughout the simulations, the channel assumed is Rayleigh faded with $E[|h_{S_1S_2}|^2] = E[|h_{S_1R}|^2] = E[|h_{RS_1}|^2] = 1$. We simulate the system for two scenarios, assuming channels from the relay to both sources have the same power (i.e. $E[|h_{S_2R}|^2] = E[|h_{RS_2}|^2] = 1$), and assuming that one source is closer to the relay than the other (we chose the value of $E[|h_{S_2R}|^2] = E[|h_{RS_2}|^2] = 1/16$). In order to maintain the same notation with previous simulation results, we define the x-axis as $\bar{\gamma} = \frac{E_b}{N_0}$ for the rest of the simulation results.

4.4.1 Symmetric Source-Relay Channels

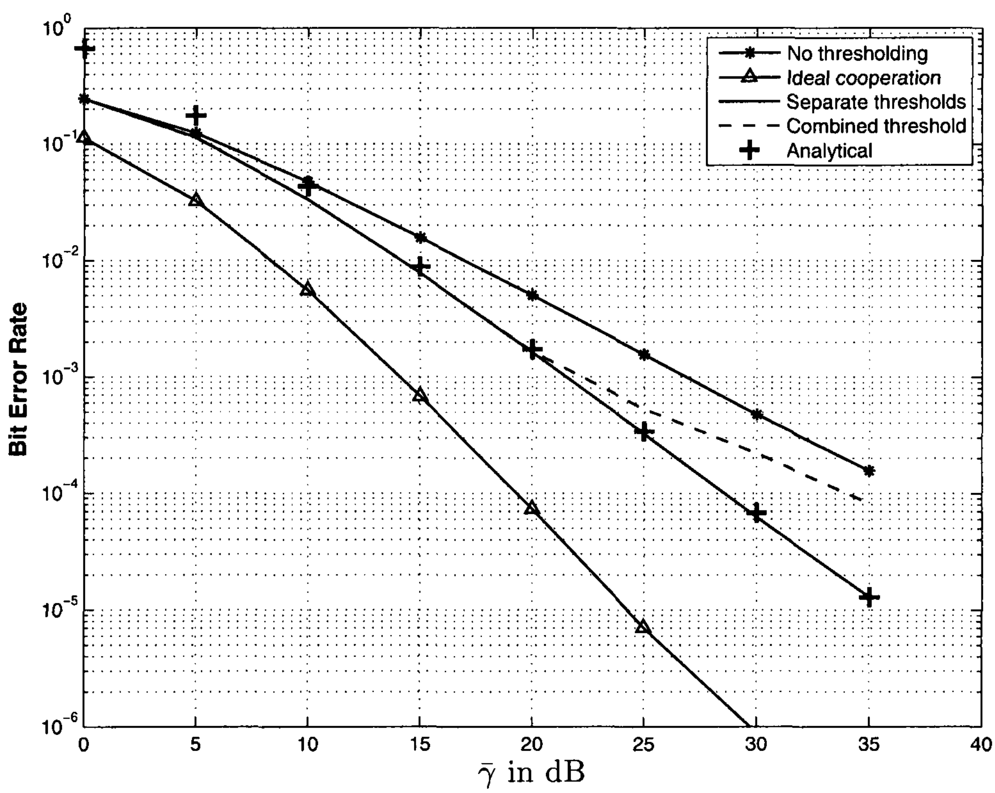

Figure 4.2: Bit error rate vs. $\bar{\gamma}$, for $E[|h_{S_2R}|^2] = E[|h_{RS_2}|^2] = 1$.

The results of the simulations for this case are displayed in Fig. 4.2. We display one set of bit error rate curves since $P_{S_1}^{(e)} = P_{S_2}^{(e)}$ for this case. In the figure, we can notice a complete loss of diversity in the case of no thresholding (diversity of 1 is observed), in contrast with the case of ideal cooperation where a diversity of 2 is shown. We can see the significant diversity gain that separate thresholds provides over no thresholding at the relay, with the performance of separate thresholds displaying a gain of more than 10 dB at BER = 10^{-4} over no thresholding. Although we see a matching performance of combined thresholding for $\bar{\gamma} < 20dB$, we notice that after that point the performance of combined thresholding becomes worse than separate thresholds; attributed to it resulting in more bits being nulled which prevents diversity gains. Finally, we note the matching of analytical and simulation for the optimized separate thresholds at $\bar{\gamma} > 15dB$.

4.4.2 Asymmetric Source-Relay Channels

In this case, we set $E[|h_{RS_2}|^2] = 1/16$ to introduce asymmetry in the system model. Hence, both the uplink and downlink from/to S_2 degrades relative to the uplink and downlink from/to S_1–impacting the correct detection of y_1 at S_2.

For this case, results are presented in terms of bit error rates $P_{S_1}^{(e)}, P_{S_2}^{(e)}$ since they are not equal. As such, we note that for this case we have four variants of thresholding at the relay: Optimizing separate thresholds at the relay for minimum $P_{S_1}^{(e)}$, doing so for minimum $P_{S_2}^{(e)}$, optimizing one combined threshold at the relay for minimum $P_{S_1}^{(e)}$, and optimizing one combined threshold for minimum $P_{S_2}^{(e)}$. We found the optimal threshold(s) for all cases (as outlined in Section 4.3) and simulated the performance of the system for each case. We compare the performance of all four variants in Fig. 4.3. We first notice that, in general, $P_{S_1}^{(e)} > P_{S_2}^{(e)}$; highlighting the impact of incorrect

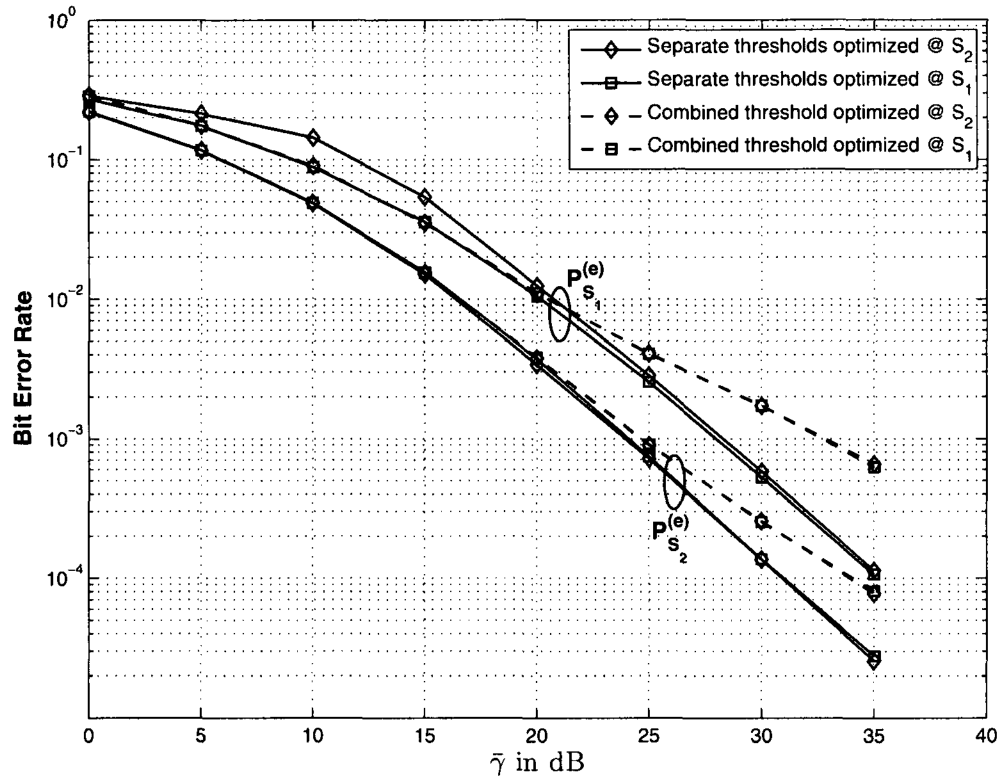

Figure 4.3: Comparison of different thresholding case for asymmetric source-relay channels, $\left(P_{S_1}^{(e)}, P_{S_2}^{(e)}\right)$ vs. $\bar{\gamma}$, for $E[|h_{S_2R}|^2] = E[|h_{RS_2}|^2] = 1/16$.

detection at the relay. In addition, for $\bar{\gamma} < 20dB$ we see that the difference between all four cases is negligible in both $P_{S_1}^{(e)}$ and $P_{S_2}^{(e)}$. As an example, we see that $P_{S_1}^{(e)}$ using separate thresholds optimized for S_2 is slightly worse than when these thresholds are optimized for S_1. For $\bar{\gamma} > 20dB$ however, we see that combined thresholding loses diversity and performs worse than separate thresholds– a behavior observed in the case of symmetric source-relay channels as well.

To show the improvement of using thresholding, we display the results for simulating the cases of no thresholding and perfect cooperation at the relay, along with the performance of optimized separate[1] thresholds in Fig. 4.4. We point that $P_{S_1}^{(e)} > P_{S_2}^{(e)}$

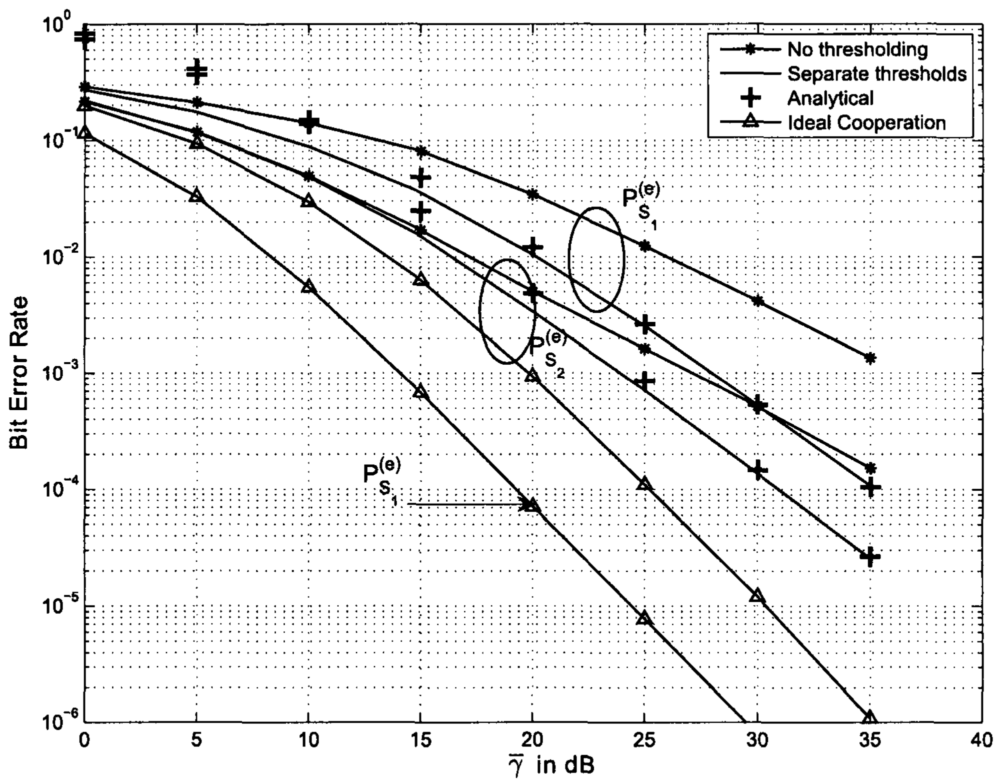

Figure 4.4: Bit error rate$\left(P_{S_1}^{(e)}, P_{S_2}^{(e)}\right)$ vs. $\bar{\gamma}$, for asymmetric source-relay channels where $E[|h_{S_2R}|^2] = E[|h_{RS_2}|^2] = 1/16$.

(except with ideal cooperation where the bit error rate depends only on the downlink channel). Moreover, we see a gain very similar to the one observed in the symmetric

[1] We chose to display the performance of separate thresholds since we can calculate all components of $P_{S_1}^{(e)}$,$P_{S_2}^{(e)}$, while for the case of a combined threshold we did not obtain a closed-form expression for $f_{z_\oplus}(z)$

case, with higher diversity achieved by thresholding. Interestingly, the gain achieved by thresholding is greater for $P_{S_1}^{(e)}$ (where the performance without thresholding is significantly worse) than $P_{S_2}^{(e)}$; we note that even $P_{S_1}^{(e)}$ with thresholding becomes lower than $P_{S_2}^{(e)}$ without thresholding. We observe gains up to $8dB$ for $P_{S_1}^{(e)}$, and up to $5dB$ for $P_{S_21}^{(e)}$. Finally we see that the analytical expression for the performance with thresholding matches at $\tilde{\gamma} > 20dB$.

4.5 Extension to Channel-Coded Network-Coded Scenarios

We can allow the cooperative system under study to adopt the same channel coding scheme detailed in Chapter 3. In this section we briefly discuss issues in extending thresholding to a channel-coded, network-coded system.

4.5.1 System Model

Analogous to the system model in this chapter, we modify (4.1)-(4.4) to use channel coding, hence the output of each terminal during the broadcast stage becomes

$$\begin{aligned}
r_{S_1R}[n] &= \sqrt{R_{c_1}E_b}h_{S_1R}[n]y_{S_1}[n] + n_{S_1R}[n], \\
r_{S_2R}[n] &= \sqrt{R_{c_1}E_b}h_{S_2R}[n]y_{S_2}[n] + n_{S_2R}[n], \\
r_{S_1S_2}[n] &= \sqrt{R_{c_1}E_b}h_{S_1S_2}[n]y_{S_1}[n] + n_{S_1S_2}[n], \\
r_{S_2S_1}[n] &= \sqrt{R_{c_1}E_b}h_{S_2S_1}[n]y_{S_1}[n] + n_{S_2S_1}[n],
\end{aligned}$$

where $y_{S_1}[n]$ and $y_{S_2}[n]$ denote the coded bits transmitted by S_1 and S_2, respectively, where the same channel coding used in Chapter 3 is used to obtain $y_{S_1}[n]$ and $y_{S_2}[n]$, and $n = 1, 2, \ldots, N/R_{c_1}$. Moreover, during the cooperation stage we can modify (4.5) and (4.6) (for the case of individual thresholding) as

$$\begin{aligned} r_{RS_1}[n] &= \sqrt{R_{c2}\frac{E_b}{2}}h_{RS_1}[n]\hat{u}_{\oplus}[n] + n_{RS_1}[n], \\ r_{RS_2}[n] &= \sqrt{R_{c2}\frac{E_b}{2}}h_{RS_2}[n]\hat{u}_{\oplus}[n] + n_{RS_2}[n], \end{aligned}$$

respectively, where $\hat{u}_{\oplus}[n] = \hat{u}_{S_1}[n] \oplus \hat{u}_{S_2}[n] = -\left(\hat{u}_{S_1}[n]\hat{u}_{S_2}[n]\right)$ where $\hat{u}_{S_1}[n]$ and $\hat{u}_{S_2}[n]$ are the modulated output of the relay for the bits of S_1 and S_2, respectively, and $n = N/R_{c_1}1, \ldots, \left(\frac{1}{R_{c_1}} + \frac{1}{R_{c_2}}\right)N$. However, during the cooperation stage the sources are also transmitting (hence the division of power by 2), whose output is expressed–for the cooperation stage–as

$$\begin{aligned} r_{S_2S_1}[n] &= \sqrt{R_{c2}\frac{E_b}{2}}h_{S_2S_1}[n]u_{S_2}[n] + n_{RS_1}[n], \\ r_{S_1S_2}[n] &= \sqrt{R_{c2}\frac{E_b}{2}}h_{S_1S_2}[n]u_{S_1}[n] + n_{RS_2}[n], \end{aligned}$$

Finally, both sources combine their respective copies of the cooperation stage frames as

$$\begin{aligned} r_{\text{MRC},S_1}[n] &= h^*_{S_2S_1}[n]r_{S_2S_1}[n] - u_{S_1}[n]h^*_{RS_1}[n]r_{RS_1}[n], \\ r_{\text{MRC},S_2}[n] &= h^*_{S_1S_2}[n]r_{S_1S_2}[n] - u_{S_2}[n]h^*_{RS_2}[n]r_{RS_2}[n]. \end{aligned}$$

At each source, decoding is carried out in the same way described in Section 3.1.4 to obtain the decided bits.

4.5.2 Thresholding Protocol

As simulation results (see Section 4.4) have proven earlier, thresholding done at the individual-bit level yields better results than at the combined-bit level. Thus, we only consider thresholding done on individual-bits at the relay. We have already obtained optimal individual thresholds for a single channel-coded cooperative system in Chapter 3. Hence, the thresholding rule can be formally defined as

$$\hat{u}_{\oplus} = \begin{cases} -\left(\hat{u}_{S_1}\hat{u}_{S_2}\right), & \left|\Lambda_{\hat{u}_{S_1}}\right| > T_{S_1} \text{ and } \left|\Lambda_{\hat{u}_{S_2}}\right| > T_{S_2} \\ 0, & \text{otherwise} \end{cases}.$$

where $\Lambda_{\hat{u}_{S_1}}$ and $\Lambda_{\hat{u}_{S_2}}$ are obtained at the relay from decoding r_{S_1R} and r_{S_2R}, respectively, using a SISO decoder.

4.5.3 System Analysis

To shed some light on analyzing the performance of the system in this case, we exploit a convenient property of network-coded cooperative systems. Namely, that any network-coded bit that was erroneously forwarded is equivalent to both sources receiving an erroneous bit from the relay. Similarly, a nulled network-coded bit will translate into a nulled bit for both sources.

Recalling the final PEP expression for a single, channel-coded cooperative system obtained in (3.21), we can substitute d_E, d_R by $d_{E_{XOR}}, d_{R_{XOR}}$ to indicate the number of bits in the *combined* forwarded frame in error and nulled, respectively. Hence, (3.21) becomes

$$P(d) = \sum_{d_R=0}^{d_{R_1}+d_{R_2}} \sum_{d_E=0}^{d_{E_1}+d_{E_2}} \sum_{d_r=0}^{d_2} \sum_{d_e=0}^{d_r} \Big[P(d|d_e, d_r = d_c + d_e) p_{d_e}(d_e|d_{E_{XOR}}, d_{R_{XOR}}) p_{d_r}(d_r|d_{R_{XOR}}) \\ p_{d_{E_{XOR}}}(d_{E_{XOR}}) p_{d_{R_{XOR}}}(d_{R_{XOR}}) \Big], \tag{4.19}$$

which can apply to the bit error rate at any source by substituting the appropriate SNR, where d_{E_1} and d_{E_2} are the number of bits in error in the decoded frames of S_1 and S_2, respectively. We can see from (4.19) that we have two unknown PDFs– $p_{d_{E_{XOR}}}(d_{E_{XOR}})$ and $p_{d_{R_{XOR}}}(d_{R_{XOR}})$. To obtain them, we write $d_{E_{XOR}}$ and $d_{R_{XOR}}$ as

$$\begin{aligned} d_{R_{XOR}} &= d_{R_1} + d_{R_2} - d_{R_{COM}}, \\ d_{E_{XOR}} &= d_{E_1} + d_{E_2} - 2d_{E_{COM}}, \end{aligned}$$

where $d_{R_{COM}}$ indicates the number of bits commonly nulled in both decoded frames at the relay, and similarly for $d_{E_{COM}}$. Hence, $p_{d_{E_{XOR}}}(d_{E_{XOR}})$ and $p_{d_{R_{XOR}}}(d_{R_{XOR}})$ can be written in terms of the underlying PDFs as

$$
\begin{aligned}
p_{d_{R_{XOR}}}(d_{R_{XOR}}) &= \sum_{\substack{\forall d_{R_1}, d_{R_2}, d_{R_{COM}}: \\ d_{R_{XOR}} = d_{R_1} + d_{R_2} - d_{R_{COM}}}} p_{d_{R_1}}(d_{R_1}) p_{d_{R_2}}(d_{R_2}) p_{d_{R_{COM}}}(d_{R_{COM}} | d_{R_1}, d_{R_2}), \\
p_{d_{E_{XOR}}}(d_{E_{XOR}}) &= \sum_{\substack{\forall d_{E_1}, d_{E_2}, d_{E_{COM}}: \\ d_{E_{XOR}} = d_{E_1} + d_{E_2} - 2d_{E_{COM}}}} p_{d_{E_1}}(d_{E_1}) p_{d_{E_2}}(d_{E_2}) p_{d_{E_{COM}}}(d_{E_{COM}} | d_{E_1}, d_{E_2}),
\end{aligned}
$$

Then, assuming that the positions of errors and nulls at the decoded frames are independent, we can express $p_{d_{R_{COM}}}(d_{R_{COM}} | d_{R_1}, d_{R_2})$ and $p_{d_{E_{COM}}}(d_{E_{COM}} | d_{E_1}, d_{E_2})$ as

$$
p_{d_{R_{COM}}}(d_{R_{COM}} | d_{R_1}, d_{R_2}) = \begin{cases} \dfrac{\binom{2N}{d_{R_{COM}}}\binom{2N-d_{R_{COM}}}{d_{R_1}-d_{R_{COM}}}\binom{2N-d_{R_{COM}}}{d_{R_2}-d_{R_{COM}}}}{\binom{2N}{d_{R_1}}\binom{2N}{d_{R_2}}}, \\ \min(d_{R_1}, d_{R_2}) > d_{R_{COM}} > 0 \\ \dfrac{\binom{2N}{\max(d_{R_1}, d_{R_2})}\binom{2N-\max(d_{R_1}, d_{R_2})}{\min(d_{R_1}, d_{R_2})}}{\binom{2N}{d_{R_1}}\binom{2N}{d_{R_2}}}, \\ d_{R_{COM}} = 0, 2N - \max(d_{R_1}, d_{R_2}) \geq \min(d_{R_1}, d_{R_2}) \end{cases}
$$

$$
p_{d_{E_{COM}}}(d_{E_{COM}} | d_{E_1}, d_{E_2}) = \begin{cases} \dfrac{\binom{2N}{d_{E_{COM}}}\binom{2N-d_{E_{COM}}}{d_{E_1}-d_{E_{COM}}}\binom{2N-d_{E_{COM}}}{d_{E_2}-d_{E_{COM}}}}{\binom{2N}{d_{E_1}}\binom{2N}{d_{E_2}}}, \\ \min(d_{E_1}, d_{E_2}) > d_{E_{COM}} > 0 \\ \dfrac{\binom{2N}{\max(d_{E_1}, d_{E_2})}\binom{2N-\max(d_{E_1}, d_{E_2})}{\min(d_{E_1}, d_{E_2})}}{\binom{2N}{d_{E_1}}\binom{2N}{d_{E_2}}}, \\ d_{E_{COM}} = 0, 2N - \max(d_{E_1}, d_{E_2}) \geq \min(d_{E_1}, d_{E_2}) \end{cases}
$$

Finally, the rest of the underlying PDFs are defined similar to the definitions in

Subsection 3.3.2, namely,

$$p_{d_r}(d_r|d_{R_{XOR}}) = \frac{\binom{d_2}{d_r}\binom{2N-d_2}{d_{R_{XOR}}-d_r}}{\binom{2N}{d_{R_{XOR}}}}, \quad p_{d_e}(d_e|d_{R_{XOR}}, d_{E_{XOR}}) = \frac{\binom{d_r}{d_e}\binom{d_{R_{XOR}}-d_r}{d_{E_{XOR}}-d_e}}{\binom{d_{R_{XOR}}}{d_{E_{XOR}}}},$$

$$p_{d_{E_1}}(d_{E_1}) = \mathcal{B}\left(d_{E_1}, N/R_{c2}, \frac{\bar{d}_{E_1}}{N/R_{c_2}}\right), p_{d_{C_1}}(d_{C_1}) = \mathcal{B}\left(d_{C_1}, N/R_{c2}, \frac{\bar{d}_{C_1}}{N/R_{c_2}}\right)$$

$$p_{d_{R_1}}(d_{R_1} = d_{C_1} + d_{E_1}) = p_{d_{C_1}}(d_{C_1}) * p_{d_{E_1}}(d_{E_1}),$$

$$p_{d_{E_2}}(d_{E_2}) = \mathcal{B}\left(d_{E_2}, N/R_{c2}, \frac{\bar{d}_{E_2}}{N/R_{c_2}}\right), p_{d_{C_2}}(d_{C_2}) = \mathcal{B}\left(d_{C_2}, N/R_{c2}, \frac{\bar{d}_{C_2}}{N/R_{c_2}}\right)$$

$$p_{d_{R_2}}(d_{R_2} = d_{C_2} + d_{E_2}) = p_{d_{C_2}}(d_{C_2}) * p_{d_{E_2}}(d_{E_2}),$$

where $\bar{d}_{C_1}$,$\bar{d}_{C_2}$,$\bar{d}_{E_1}$, and $\bar{d}_{E_2}$ are controlled by CSI thresholds set individually by the relay for the decoded frames of S_1 and S_2.

4.5.4 Optimizing the Threshold at the Relay

We can optimize the threshold for this case in an analogous fashion to the threshold optimization procedure in 3.4.1. That is, we find the region of possible $\left(\bar{d}_{C_1}, \bar{d}_{C_2}, \bar{d}_{E_1}, \bar{d}_{E_2}\right)$ tuples, we evaluate (4.19) for each point, using all underlying PDFs found earlier, and we choose the operational point that leads to the minimum bit error rate. In this case however, we can substitute the related values in (4.19) to evaluate the bit error rate at S_1 or S_2, which leads to optimizing the thresholds w.r.t that bit error rate.

As a proof of concept, we assume a symmetric system, where $\bar{\gamma}_{S_1R} = \bar{\gamma}_{S_2R}$. Hence, optimizing the thresholds reduces to optimizing a single threshold w.r.t a single bit error rate.

Through following the same procedure set and used in Section 3.4.1, we found the optimal values for the case when all channels experience quasi-static fading and

$$\bar{\gamma}_{S_1R} = \bar{\gamma}_{S_2R} = \bar{\gamma}_{RS_1} = \bar{\gamma}_{RS_2} = \bar{\gamma}_{S_1S_2} = \bar{\gamma}_{S_2S_1}.$$

4.5.5 Simulation Results

All Quasi-Static Channels

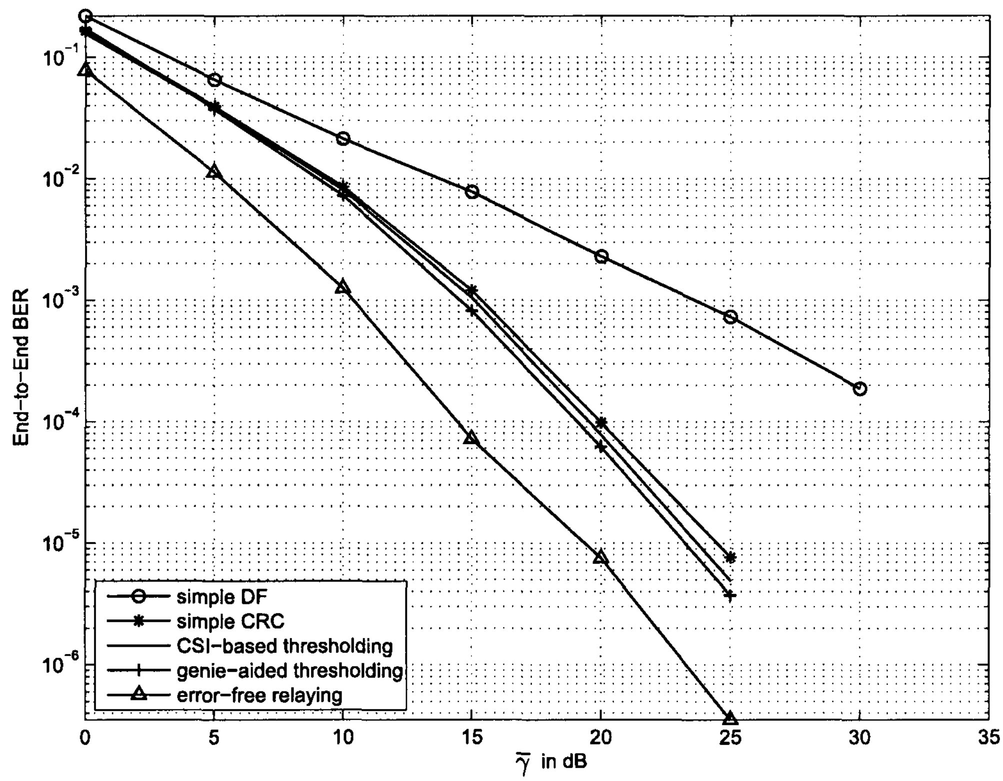

Figure 4.5: Bit error rate $\left(P_{S_1}^{(e)} = P_{S_2}^{(e)}\right)$ vs. $\bar{\gamma}$, for symmetric source-relay channels where $E[|h_{S_2R}|^2] = E[|h_{RS_2}|^2] = 1$, and all channels are modeled as quasi-static.

In this case, we simulate the system with all channels exhibiting quasi-static fading. The results of the simulations for this case are displayed in Fig. 4.5. We display one set of bit error rate curves since $P_{S_1}^{(e)} = P_{S_2}^{(e)}$. In the figure, we can notice a complete loss of diversity in the case of no thresholding (diversity of 1 is observed), in contrast with the case of ideal cooperation where a diversity of 2 is shown. We can see the significant diversity gain that thresholding provides over no thresholding at the relay, with the performance of thresholding displaying a gain of more than 10 dB at BER $= 10^{-4}$ over no thresholding. We also see that the performance of simple CRC is very close to thresholding (both genie-aided and CSI-based); which is to be expected in the case of quasi-static channels.

Block-Faded/Quasi-Static Channels

In this case, we simulate the system with the inter-source channel exhibiting quasi-static fading, while the rest of the channels exhibit block fading. The results of the simulations for this case are displayed in Fig. 4.6. Similar to the previous case, we notice a loss of diversity in the case of no thresholding, in contrast with the case of ideal cooperation where a diversity of 2 is shown. We can see the significant diversity gain that thresholding provides over no thresholding at the relay. In contrast with the previous case, we see that the performance of simple CRC is much worse than thresholding; which results from higher diversity in the source-relay channels. For instance, the performance of thresholding displaying a gain over CRC of around 7 dB at BER $= 10^{-4}$.

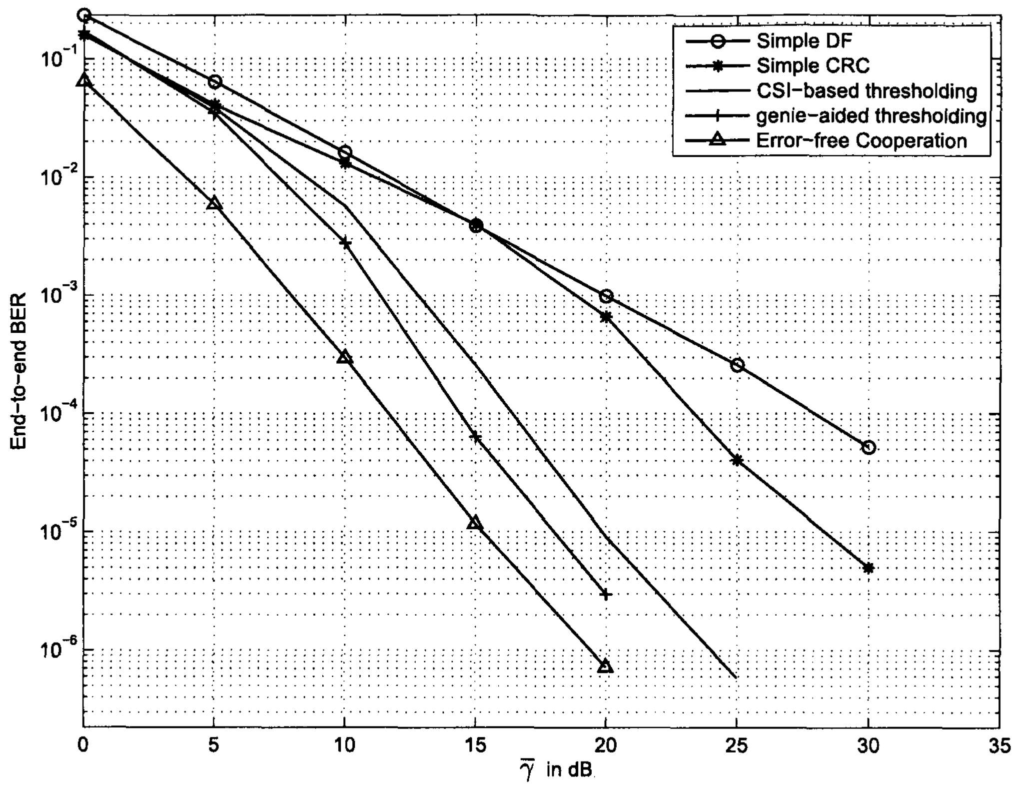

Figure 4.6: Bit error rate $\left(P_{S_1}^{(e)} = P_{S_2}^{(e)}\right)$ vs. $\bar{\gamma}$, for symmetric source-relay channels where $E[|h_{S_2R}|^2] = E[|h_{RS_2}|^2] = 1$, and the inter-source channel is modeled as quasi-static fading, and source-relay channels are modeled as block fading.

All Block-Faded Channels

In this case, we simulate the system with all channels exhibiting block fading. The results of the simulations for this case are displayed in Fig. 4.7. In the figure, we observe similar trends to the previous case, with higher diversity rates achieved due to the inter-source channel becoming more diverse.

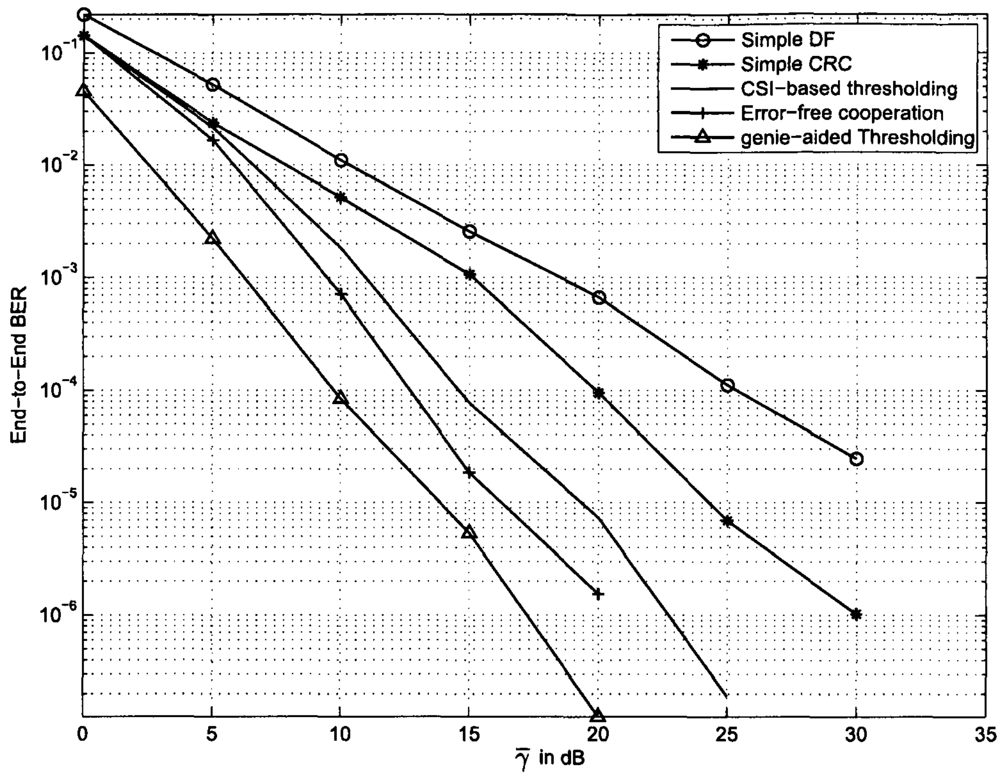

Figure 4.7: Bit error rate $\left(P_{S_1}^{(e)} = P_{S_2}^{(e)}\right)$ vs. $\bar{\gamma}$, for symmetric source-relay channels where $E[|h_{S_2R}|^2] = E[|h_{RS_2}|^2] = 1$, and all channels are modeled as block fading.

4.6 Conclusion

In this chapter, we have extended the proposed thresholding technique to network-coded cooperative communication systems. We analyzed the performance of the proposed system and optimized the threshold for different cases of thresholding. When compared with using no thresholding at the relay, the proposed thresholding displayed significant improvement in performance. Finally, we investigated applying thresholding to channel-coded network-coded cooperative communication systems. We displayed significant performance improvement in a channel-coded system as well.

Chapter 5

Conclusion

5.1 Concluding Remarks

In this thesis, we have presented a technique that aims at mitigating error propagation in cooperative communications. Our proposed system relied on soft estimates of bits, generated using a SISO decoder at the relay, as reliability measures and used them to decide whether a bit is reliable enough or not, forwarding it to the destination accordingly. We compared our system with just using CRC at the relay, with simple DF, and analog LLR forwarding and displayed significant improvement in diversity and bit error rate. While analog LLR forwarding and simple DF cause an error floor in the end-to-end bit error rate of the system, CRC loses diversity as well by discarding the whole frame. We discussed two types of thresholding at the relay– genie-aided and CSI-based. Through analysis and simulations we demonstrated how the threshold can mitigate the adverse effects of CRC and analog LLR forwarding, and approach the ideal (error-free) performance of the cooperative system. By touching briefly on the case where the relay-destination channel becomes more diverse, we demonstrated that the efficacy of competing schemes is reduced as the relay-destination channel becomes more diverse. Finally, observing the still existent performance gap between the proposed threshold and the error-free performance, we are lead to believe a better thresholding scheme at the relay can be developed, possibly incorporating adaptive elements and/or extra processing at the relay.

Furthermore, we have extended the proposed technique to network-coded cooperative network. We analyzed the performance of the proposed system and optimized the threshold for different cases of thresholding, namely, thresholds applied separately and applied on the combined bits. We compared our technique with using no thresholding at the relay and displayed significant improvement in performance. We concluded that even in cases where the relay-source channels are asymmetric, optimizing the thresholds for either BER does not change the resultant thresholds much. In addition, we observed that using separate thresholds yields better performance than using combined thresholding.

5.2 Future Work

Throughout the presented simulation results, we can see a significant gap between achieved performance and error-free performance. This leads us to believe that further performance improvement can be achieved through more sophisticated thresholding. That said, further expansion on the developed scheme is possible to bring it closer to practical application in cooperative systems. A few areas where further research and expansion of the presented work are shown below

- The scheme can be expanded to use higher-order modulation; seeing that most practical standards define higher-order modulation for their air interfaces. The challenge would thus be to specify would symbol would be transmitted (if any), given that one of its constituent bits was nulled.

- Variants to the coding/decoding parts of the system can be investigated. Specifically, the effect of different channel codes, code rates, and SISO decoders can be analyzed.

- Expanding the system to multiple relays can make the system more applicable to mesh networks, where typically a large number of nodes are available to cooperate with the source.

- The proposed threshold relied on a linear relationship with the observed CSI only. We believe that adding more criteria to the threshold can result in better end-to-end performance.

- The sensitivity of the threshold's performance to imperfect channel estimation can be investigated; leading to a more practical analysis of the system.

Bibliography

[1] Y. Li, B. Vucetic, T. F. Wong, and M. Dohler, "Distributed turbo coding with soft information relaying in multihop relay networks," *IEEE J. Sel. Areas Commun.*, vol. 24, pp. 2040–2050, Nov. 2006.

[2] S. V. Alamouti, "A simple transmit diversity technique for wireless communications," *IEEE J. Sel. Areas Commun.*, vol. 16, pp. 1451–1458, Oct. 1998.

[3] G. Foschini and M. Gans, "On the limits of wireless communications in a fading environment when using multiple antenna," *Wireless Personal Communications*, vol. 6, pp. 311–335, Mar. 1998.

[4] E. Telatar, "Capacity of multi-antenna gaussian channels," Jun. 1995, AT&T Bell Labs Internal Memo.

[5] A. Sendonaris, E. Erkip, and B. Aazhang, "User cooperation diversity. part i: System description and part ii: Implementation aspects and performance analysis," *IEEE Trans. Commun.*, vol. 51, pp. 1927–1948, Nov. 2003.

[6] R. U. Nabar and H. Bolcskei, "Space-time signal design for fading relay channels," in *IEEE GLOBECOM*, Dec. 2003, pp. 1952–1956.

[7] R. U. Nabar, H. Bolcskei, and F. Kneubuhler, "Fading relay channels: performance limits and space-time signal design," *IEEE J. Sel. Areas Commun.*, vol. 22, pp. 1099–1109, Aug. 2004.

[8] D. Chen and J. N. Laneman, "Modulation and demodulation for cooperative diversity in wireless systems," *IEEE Trans. Wireless Commun.*, vol. 5, pp. 1785–1794, Jul. 2006.

[9] J. N. Laneman, D. N. C. Tse, and G. W. Wornell, "Cooperative diversity in wireless networks: Efficient protocols and outage behavior," *IEEE Trans. Inf. Theory*, vol. 50, pp. 3062–3080, Dec. 2004.

[10] G. Kramer, M. Gastpar, and P. Gupta, "Cooperative strategies and capacity theorems for relay networks," *IEEE Trans. Inf. Theory*, vol. 51, pp. 3037–3063, Sep. 2005.

[11] I. Abou-Faycal and M. Médard, "Optimal uncoded regeneration for binary antipodal signaling," in *Proc. IEEE International Conference on Communications, ICC*, Jun. 2004, pp. 742–746.

[12] L. Lai, K. Liu, and H. E. Gamal, "The three-node wireless network: Achievable rates and cooperation strategies," *IEEE Trans. Inf. Theory*, vol. 52, pp. 805–828, Mar. 2006.

[13] K. S. Gomadam and S. A. Jafar, "Optimal relay functionality for snr maximization in memoryless relay networks," *IEEE J. Sel. Areas Commun.*, vol. 25, pp. 390–401, Feb. 2007.

[14] M. Elfituri, W. Hamouda, and A. Ghrayeb, "A convolutional-based coded cooperation scheme for relay channels," *IEEE Trans. Veh. Technol.*, accepted for publication, May 2008.

[15] T. Hunter and A. Nosratinia, "Diversity through coded cooperation," *IEEE Trans. Wireless Commun.*, vol. 5, pp. 283–289, Feb. 2006.

[16] J. P. K. Chu, R. S. Adve, and A. W. Eckford, "Relay selection for low-complexity coded cooperation using the bhattacharyya parameter," in *Proc. IEEE International Conference on Communications, ICC*, May 2008, pp. 1008–1012.

[17] B. Zhao and M. Valenti, "Distributed turbo coded diversity for relay channel," *Electronics Letters*, vol. 39, pp. 786–787, May 2003.

[18] Z. Zhang and T. M. Duman, "Capacity-approaching turbo coding and iterative decoding for relay channels," *IEEE Trans. Commun.*, vol. 53, pp. 1895–1905, Nov. 2005.

[19] M. N. Khormuji and E. G. Larsson, "Improving collaborative transmit diversity by using constellation rearrangement," in *Proc. IEEE Wireless Communications and Networking Conference, WCNC*, Mar. 2007, pp. 803–807.

[20] H. V. Khuong and H. Y. Kong, "LLR-based decode-and-forward protocol for relay networks and closed-form ber expressions," *IEICE Trans. Fundamentals*, vol. E89A, pp. 1832–1841, Jun. 2006.

[21] R. C. Palat, A. Annamalai, and J. H. Reed, "Log-likelihood-ratio based selective decode and forward cooperative communication," in *Proc. IEEE Vehicular Technology Conference, VTC*, May 2008, pp. 615–618.

[22] T. W. S. L. K. Siriwongpairat, W.P.; Himsoon, "Optimum threshold-selection relaying for decode-and-forward cooperation protocol," in *Proc. IEEE Wireless Communications and Networking Conference, 2006. WCNC 2006.*, Apr. 2006, pp. 1015–1020.

[23] M. N. Khormuji and E. G. Larsson, "Receiver design for wireless relay channels with regenerative relays," in *Proc. IEEE International Conference on Communications, ICC*, Jun. 2007, pp. 4034–4039.

[24] M. R. Souryal and B. R. Vojcic, "Performance of amplify-and-forward and decode-and-forward relaying in rayleigh fading with turbo codes," in *Proc. IEEE International Conference on Acoustics, Speech and Signal Processing.ICASSP*, May 2006, pp. IV–IV.

[25] Y. Hairej, A. Darmawan, and H. Morikawa, "Cooperative diversity using soft decision and distributed decoding," in *Proc. Mobile and Wireless Communications Summit*, Nagoya, Japan, Jul. 2007, pp. 1–5.

[26] A. Chakrabarti, A. de Baynast, A. Sabharwal, and B. Aazhang, "Half-duplex estimate-and-forward relaying: Bounds and code design," in *Proc. IEEE International Symposium on Information Theory*, Jul. 2006, pp. 1239–1243.

[27] R. Ahlswede, N. Cai, S.-Y. R. Li, and R. W. Yeung, "Network information flow," *IEEE Trans. Inf. Theory*, vol. 46, pp. 1204–1216, Jul. 2000.

[28] S.-Y. R. Li, R. W. Yeung, and N. Cai, "Linear network coding," *IEEE Trans. Inf. Theory*, vol. 49, pp. 371–381, Feb. 2003.

[29] R. Koetter and M. Medard, "An algebraic approach to network coding," *IEEE/ACM Transactions on Networking*, vol. 11, pp. 782–795, Oct. 2003.

[30] E. G. Larrson and B. R. Vojcic, "Cooperative transmit diversity based on superposition modulation," *IEEE Commun. Lett.*, vol. 9, pp. 778–780, Sep. 2005.

[31] L. Xiao, T. E. Fuja, J. Kliewer, and D. Costello, "A network coding approach to cooperative diversity," *IEEE Trans. Inf. Theory*, vol. 53, pp. 3714–3722, Oct. 2007.

[32] C. Hausl and J. Hagenauer, "Iterative network and channel decoding for the two-way relay channel," in *Proc. IEEE Internation Conference on Communications, ICC*, Jun. 2006, pp. 1568–1573.

[33] S. Zhang, Y. Zhu, S.-C. Liew, and K. B. Letaief, "Joint design of network coding and channel decoding for wireless networks," in *Proc. IEEE Wireless Communications and Networking Conference, 2007. WCNC 2007.*, Mar. 2007, pp. 779–784.

[34] I.-J. Baik and S.-Y. Chung, "Network coding for two-way relay channels using lattices," in *Proc. IEEE International Conference on Communications. ICC '08.*, May 2008, pp. 3898–3902.

[35] K. Lu, S. Fu, and Y. Qian, "Capacity of random wireless networks: Impact of physical-layer network coding," in *Proc. IEEE International Conference on Communications. ICC '08.*, May 2008, pp. 3903–3907.

[36] C. X. Huang and A. Ghrayeb, "A simple remedy for the exaggerated extrinsic information produced by the SOVA algorithm," *IEEE Trans. Wireless Commun.*, vol. 5, pp. 996–1002, May 2006.

[37] T. M. Duman and A. Ghrayeb, *Coding for MIMO Communication Systems.* New York: Wiley, 2008.

[38] J. Proakis, *Digital Communications.* McGraw-Hill College, 2000.

[39] M. K. Simon and M.-S. Alouini, *Digital Communications Over Fading Channels: A Unified Approach to Performance Analysis.* New York: Wiley, 2000.

[40] G. Al-Habian, A. Ghrayeb, M. Hasna, and A. Abu-Dayya, "Distributed turbo coding using log-likelihood thresholding for cooperative communications," in *Proc. Asilomar Conference on Signals, Systems, and Computers*, Oct. 2008.

[41] S. W. Kim and E. Y. Kim, "Optimum receive antenna selection minimizing error probability," in *Proc. Wireless Communications and Networking Conference, WCNC*, Mar. 2003, pp. 441–447.